Mississippi State UNIVERSITY

Center for Air Sea Technology

FY96 POSTDOCTORAL ASSISTANT RESEARCH PROJECTS

Technical Report 1-97
1 December 1996

This research was supported by the Department of the Navy, Office of the Chief of Naval Research (ONR) under Research Grants N00014-95-1-0186 and N00014-959-1-0293 with MSU; Space and Naval Warfare Systems Command under NASA Contract NAS13-564 Delivery Order 73 with NRL; and through the DoD Advanced Research Projects Agency Strategic Environmental and Development Program under MSU-NSF Engineering Research Contract EEC-8907070.

Mississippi State University Center for Air Sea Technology
Stennis Space Center, MS 39529-5000

MISSISSIPPI STATE UNIVERSITY
CENTER FOR AIR SEA TECHNOLOGY

FY96
POSTDOCTORAL ASSISTANT
RESEARCH PROJECTS

BUILDING 1103-ROOM 233

STENNIS SPACE CENTER, MS 39529-6000

Compiled and Edited by
Lanny A. Yeske

This research was supported by the Department of the Navy, Office of the Chief of Naval Research (ONR) under Research Grants N00014-95-1-0186 and N00014-959-1-0293 with MSU; Space and Naval Warfare Systems Command under NASA Contract NAS13-564 Delivery Order 73 with NRL; and through the DoD Advanced Research Projects Agency Strategic Environmental and Development Program under MSU-NSF Engineering Research Contract EEC-8907070. The opinions, findings, conclusions, and recommendations expressed in this publication are those of the authors and do not necessarily reflect the views of the U.S. Government. No official endorsement should be inferred.

FOREWORD

The Center for Air Sea Technology (CAST) research program in FY96 was modified to adjust to new Navy Ocean Modeling and Prediction (NOMP) program priorities, especially in the area of coastal and semi-enclosed seas. The objectives were to:

- Conduct coastal and semi-enclosed seas ocean modeling basic research, embedded in a CAST modularized software system, with the emphasis on model relocatability to any geographical region;
- Support the technical requirements of Navy and university ocean modeling efforts by providing routine day-to-day technical support to the scientific staff, and by designing, developing, and implementing next generation technical support capability;
- Tailor and transition applicable advanced technical support capabilities developed for the research community to the operational Navy; and
- Strengthen collaboration with academia by incorporating student and faculty in CAST projects.

In accomplishing these objectives, CAST in FY1996 supported two postdoctoral assistants. This technical note summarizes the FY1996 research conducted by these individuals and their advisors. CAST was extremely pleased with the research support provided by these individuals, not only in their dedication but in the quality of the research conducted.

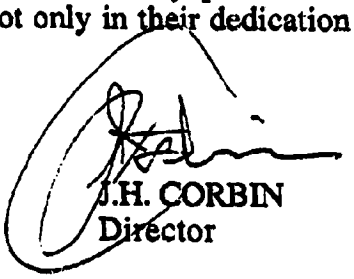

J.H. CORBIN
Director

TABLE OF CONTENTS

HIGH RESOLUTION COASTAL STUDIES
by Dr. Avichal Mehra

SCIENTIFIC ADVISOR: Dr. David Dietrich, Center for Air Sea Technology

OBJECTIVES:

To numerically model basic coastal phenomenon using accurate and efficient numerics at high resolution, and interpret them in terms of theory and observations to achieve a better understanding of the complex ocean dynamical processes involved.

APPROACH:

The z-level Mississippi State University DieCAST (Dietrich Center for Air Sea Technology) Model has emerged as very accurate and robust in application to small-scale near-coast features such as boundary currents and shelf-break fronts, and their interaction with deep water eddies. With the Navy's emphasis on coastal and shallow water regions, there is a need for high resolution models that realistically and efficiently simulate coastal ocean dynamics, including density fields and boundary currents.

The modified Arakawa "a" grid DieCAST Model is three-dimensional in a rotating frame, and uses the hydrostatic, Boussinesq, and rigid-lid approximations. It also uses flux conserving centered approximations based on control volumes and a weakly time filtered leapfrog time integration scheme.

A significant feature is that the model applies interpolations to communicate data between collocated "a" and staggered "c" grid locations. Such mixed grid approaches mitigate weak points of the respective grids(Coriolis terms on the "c" grid; "null space" pressure problems on the "a" grid). To improve grid convergence and reduce dispersion, higher order interpolations are needed. Hence, the two following modifications were introduced:

1. Reduced Dispersion Advection Scheme. The first modification involves the interpolations used for the advection terms. This scheme greatly reduces numerical dispersion, and is called the reduced dispersion advection, or "RDA", scheme. The Arakawa "a" grid model uses a "c" grid non-divergent advection velocity. The control volume"a" grid advection scheme thus requires evaluation of the fluxed quantities at the staggered "c" grid locations. Instead of using the classic linear advection scheme based on two-point averages, used by the early versions of DieCAST ocean model, the RDA

scheme includes additional information from the next nearest points which is exact for general cubic variations. The resulting interpolated field is then multiplied by the non- divergent advection velocity to get the flux at the cell face. These fluxes are then substituted into the "control volume" integrated conservation equations.

2. Modified Incompressibility Algorithm. The second modification to the ocean model involves the numerical algorithm for construction of a non-divergent advection velocity, and is referred to as the modified incompressibility algorithm, or "MIA" scheme. As with the original "a" grid scheme, the non-divergent advection velocity was determined by interpolating the "a" grid trial velocity (derived using a trial surface pressure, the hydrostatic relation and the momentum equations) to the usual "c" grid advection locations, and then "clearing out the divergence" of the resulting "c"-grid velocity by appropriate surface pressure adjustment and application. Originally, this incompressibility information was communicated back to the "a" grid locations by simply interpolating the "c" grid advection velocity back to the "a" grid locations, using the cubic spline approach in reverse. In order to take advantage of the greatly reduced numerical dispersion of the RDA scheme described above, and thus achieve low overall numerical dispersion, the reverse interpolation approach is modified. Instead of interpolating the velocity, the changes of velocity, that result from "clearing out its divergence", are interpolated. In other words, the interpolated changes are added to the original "a" grid "trial" velocity referred to above.

Combining this MIA scheme with the RDA scheme, the overall numerical dispersion is greatly reduced. The changes of velocity needed to maintain incompressibility are small compared to velocity differences at adjacent grid locations, because a good guess for the "trial" top level pressure field is available each time step from previcus results, thus producing a quasi-non-divergent velocity that requires only a small adjustment to "clear out its divergence". These new numerics are applicable to both free surface models as well as general circulation models. Much needs to be done to understand the behavior of these schemes in detail, but the results (given in the next section) show that they have interesting effects and are quite promising.

RESULTS:

The above low dispersion numerics were applied to two different studies involving distinct ocean dynamical processes. The first was the semi-enclosed basin of the Gulf of Mexico which is one of the most thoroughly observed ocean basins. It has well known mean boundary conditions, which control the internal Loop Current and eddy shedding dynamics. The Gulf is large enough to include

major ocean basin dynamic features, yet small enough to model with high resolution on workstations.

Model parameters included a lateral resolution of 1/12° and 20 vertical layers. Real unfiltered topography was used, with depths truncated at 3.5 km, and climatological winds and 30-day surface restoring to Levitus climatology were applied. Temperature-only based thermodynamics were used for the GOM study which is appropriate when deep water formation effects are secondary. Initial and inflow temperatures were based on annual mean Levitus climatology. Eastern open boundary inflow temperatures were then adjusted to give surface trapped geostrophic inflow consistent with the observed data; the corresponding inflow velocities were specified as time-constant inflows. An approximately 16 Sverdrup barotropic western boundary current inflow was specified to represent inflows from the southern Caribbean, giving a total Caribbean inflow of 25 Sverdrups. The initial velocity was zero, but inflows were switched on full strength at the first time step.

Lateral heat and momentum diffusivities were a constant 10 m-m/sec and annual mean Hellerman winds were applied for surface forcing. Vertical heat and momentum diffusivities were 1 cm-cm/sec plus a small additive variable numerical contribution. The present simulation was done on the NAVOCEANO Cray C-90 with 210 megaflops computation speed. With the 1/12° lateral resolution used on a 194 X 146 X 20 layers grid, the model simulated approximately 4 years of real GOM time per cpu-day.

The new numerics were robust in application to the propagation of warm core Loop Current eddies across the Gulf of Mexico. This propagation involved highly nonlinear dynamics: a strong front was maintained at the outer edge of the warm core eddy as it spun at about one rotation per 15 days while propagating across the Gulf of Mexico over a period of about six months (see Figure 1). Frontal eddies slowly dispersed the warm core water as it spun westward. Compared to the earlier model results, the new model results show that the warm core eddies deform more and lose their identity more rapidly because of this dispersion, but the dispersed energy appears in a much larger number of eddies, as observed.

The new modified schemes decrease numerical dispersion, and lead to tighter fronts and small scale frontal eddies (Figure 1). These can mix material across fronts, resulting in "physical" (involving resolved velocity components rather than interpolations) dispersion. Such dispersion can extend the mixing region for different water masses, leading to a more widely distributed eddy field. For small scale flow components, such as frontal eddies, such "physical" dispersion can of

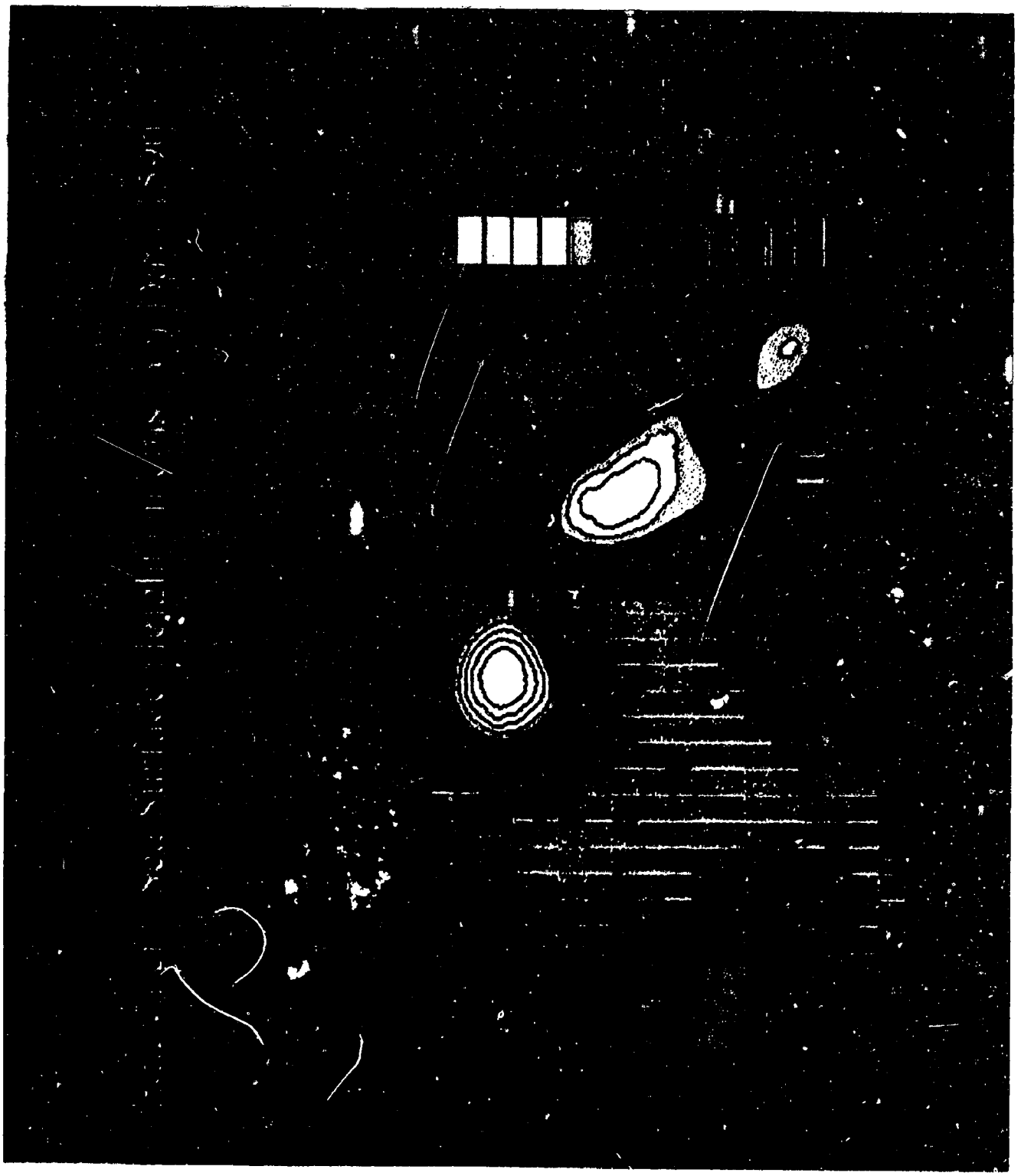

course have significant truncation error effects, yet the very existence of the frontal eddies on tight fronts is an improvement in representing nature.

The second study involved an idealized lake Kelvin wave problem to study fast (non-geostrophic) internal modes of ocean physics, specifically the transient Poincare and Kelvin wave dynamics. The computational basin was a 100 km diameter circular flat bottom lake which was 100 m deep and patterned after the Great Lakes. The domain was forced by wind which ramps up for a day and then shuts off after two days. It included the dominant geophysical dynamic effects (buoyancy and rotation) which lead to formation of Kelvin edge waves that are challenging to resolve and maintain against numerical dissipation and dispersion.

A linear equation-of-state was used with different grid resolutions of 5.00, 2.50, 1.25 and 0.6125 kms to check convergence. The new reduced dispersion scheme gave close to the correct linear Kelvin wave phase speed (about 8 days for propagation around the lake) even at coarse resolutions. The results had very small amount of dissipation as the warm front of the marginally resolved Kelvin edge wave was clearly seen for eight revolutions around the basin with only 2.5 km resolution (80 x 80 grid). (An animation of these results is available on the web site at http:\\www.cast.msstate.edu.)

The actual patterns were found to be rapidiy changing with time scales of order 1 to 8 days dominating. Initially the Poincare waves dominate the results as seen in Figure 2. But thereafter, the higher resolution low dispersion numerics cause the Kelvin wave warm front to tighten greatly after day 20 (see Figure 3). Such tightening is consistent with the fact that Kelvin wave warm fronts are much more commonly observed than cold fronts. As this happens, along-shore scale of the trailing warm water decreases rapidly until its along-shore scale roughly matches its off-shore scale, which is the natural Rossby radius of deformation. It thus becomes a half-cylinder warm core trapped against the boundary moving at the natural Kelvin wave speed.

FUTURE RESEARCH:

Plans for FY97 and FY98 include the following:

Task 1: Nested Santa Barbara Channel Model: A new high resolution Santa Barbara Channel (SBC) model, using 1/48 deg (about 2 km) resolution, will be nested inside an intermediate resolution (1/12 deg) California Current (CC) model developed in collaboration with NPS. Both will use the accurate, reduced dispersion numerics of the new DieCAST. Time permitting, the CC/SBC system will be nested in the NRL Layered Pacific Model. The initial coupling/nesting will be one-way-only, from large to small model subdomains. Time permitting, two-way coupling will be implemented in a triply nested system.

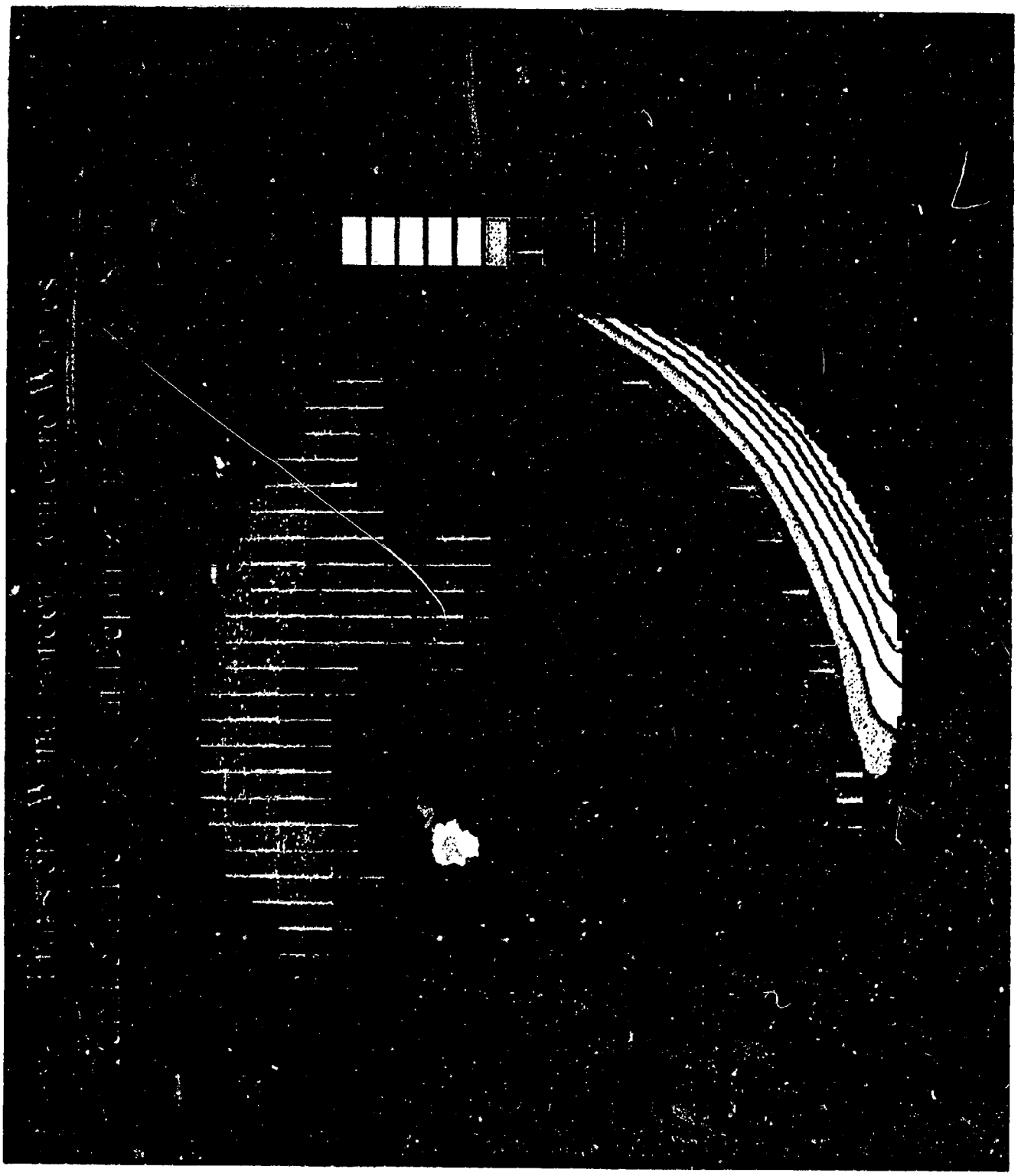

Figure 2

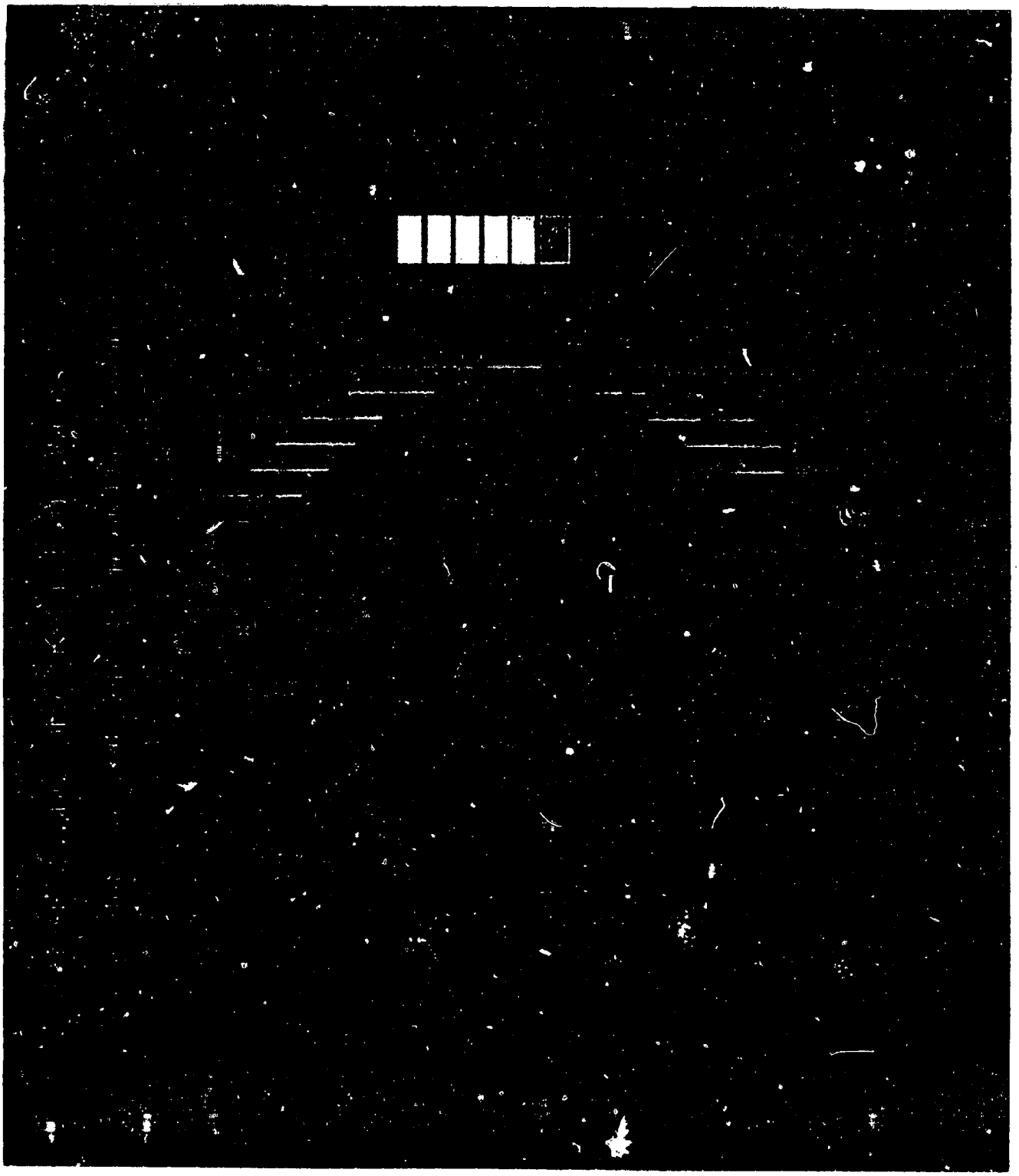

Figure 3

Larger domains will provide normal boundary velocity (nbv) conditions used by successively smaller domains in the nesting hierarchy. The nbv will be distributed non-uniformly according to the nested model internal dynamics, but the summed volume flows across a coarse resolution interface will be constrained to match the coarse resolution results. Normal boundary fluxes will be determined by the smaller domain models. A distributed jet approach may be used for the resulting momentum sources to coarser grids. Mass, momentum, temperature and salinity will be conserved by the coupling approach.

Task 2: Data Assimilation: This work will be leveraged by work done by the Minerals Management Service (MMS). The ultimate MMS goal is a nowcast/ forecast system for the California Bight Region. Thus, the work will include data assimilation into an operational version of the DieCAST model for MMS. The data assimilating DieCAST SBC model will be validated by the large SBC data base. Promising data assimilation approaches will be implemented and evaluated, as they become available, in collaboration with NPS, MIT, and Dalhousie.

Task 3: General Coastal Model: A special coastal version of DieCAST will be developed which conforms to irregular coastlines by varying the logical grid in a way such that most coastal land points will be eliminated. By shifting indices row by row, this will lead to a code with good vector and parallel computer efficiency nesting capability, for an irregular domain model which will be developed later.

Task 4: Other Applications: Idealized studies including the sensitivity of the basic phenomena in wakes from individual islands to the various parameters (steepness, Reynolds number, stratification, latitude) will be explored. These will also include island encounters with eddies advected from upstream regions, and topography effects such as steering by nearby ridges and seamounts. Also, after achieving better understanding of the basic physics of island flows, the flow dynamics around real islands in the Ryukyu island chain will be studied. The East China Sea is particularly challenging because it includes a strong boundary current along the continental shelfbreak on its west side, and also includes strong water mass transformations during wintertime. Accurate simulations requires high resolution, particularly over the shelfbreak and island chains for which large computing resources will be needed. To reduce the computing costs, we will share the computing burden by collaborating with Dr. Steve Piacsek who has developed a massively parallel version of DieCAST for the CM5. An alternative to the East China Sea is the Eastern Caribbean Sea, because of the large amount of available data, including a 1/16 resolution West Indies data set prepared by Drs. T. Townsend and A. McManus of NRL.

RELOCATABLE NUMERICAL MODELS OF MARGINAL, SEMI-ENCLOSED, AND COASTAL SEAS

by Dr. Avichal Mehra

SCIENTIFIC ADVISOR: Dr. Lakshmi Kantha, University of Colorado

TECHNICAL ADVISOR: Mr. Valentine Anantharaj, Center for Air Sea Technology

OBJECTIVE:

To develop and comprehensively test and validate increasingly complex numerical models of the coastal, marginal, and semi-enclosed seas with the entire process integrated into a relocatable modeling environment, and then transition the integrated system to the Navy's research and operational communities.

APPROACH:

Under ONR/SPAWAR sponsorship, MSU CAST and Dr. Lakshmi Kantha of the University of Colorado have developed a two-dimensional tidal model embedded in a user interactive interface that allows quick relocation of the model anywhere geographically for which databases and forcing fields exist. This model, called CURReNTSS, is a finite difference, explicit, vertically-integrated barotropic model assimilating tidal component data from coastal tide gages and from any bottom pressure gages available. It is fully non-linear and a sub- component of the NAVOCEANO/CU 3-D operational model. The model incorporates direct astronomical forcing and can also include surface forcing (winds stress and pressure fields) from atmospheric models, if available, to predict storm surges. The open boundary conditions are obtained from an earlier global run at 1/5° resolution, which are readily accessible from the GUI.

The GUI also provides bathymetry from the ETOPO5 database, which can be refined within the GUI and setup for the model. It is also possible to import bathymetry from other databases into the GUI. The model can be run with any number of components including long term and compound tides. It employs a simple data assimilation procedure by replacing the model predicted SSH at pre-determined intervals by a weighted sum of the model prediction and the observed SSH from the tide/bottom pressure at that grid point, the weights determined a priori. The tide gage data comes from the data base at the International Hydrographic Organization (1979), supplemented by the Admiralty charts (1993). This database is also available from the GUI and relevant tidal stations can be easily extracted for assimilation in the model.

CURRENTSS Model

[Winds and Pressure]

Date = 04 Jan95 03 Hr

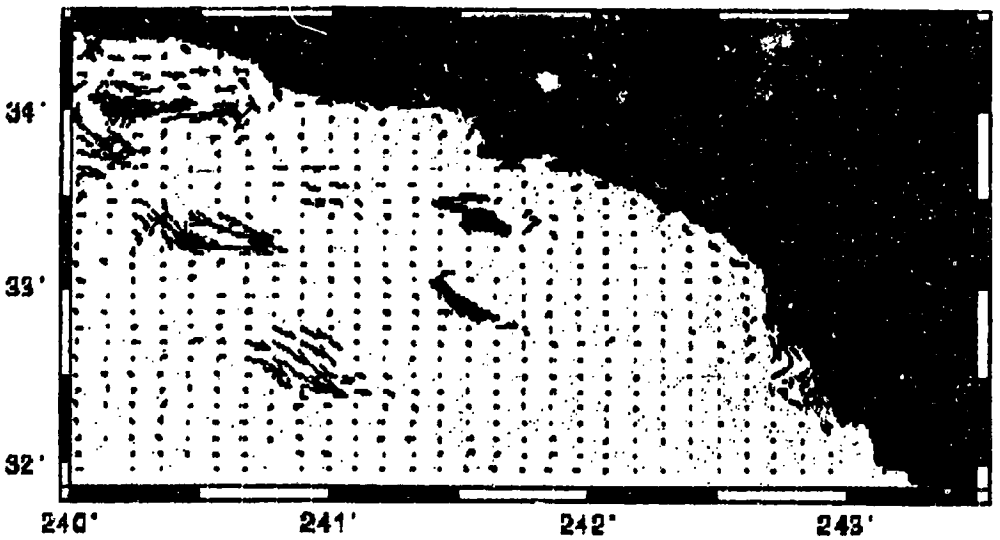

Currents

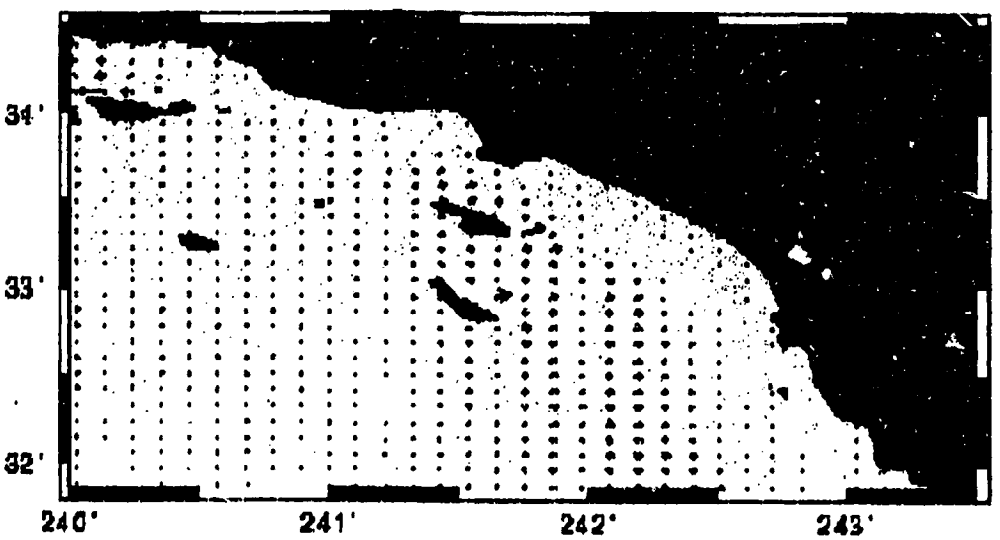

Wind Stress

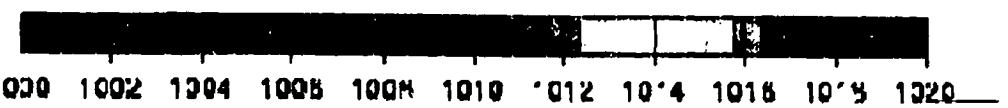

Pressure(mb)

Figure 4

CURRENTSS Model

[Winds and Pressure]

Date = 05 Jan95 23 Hr

Currents

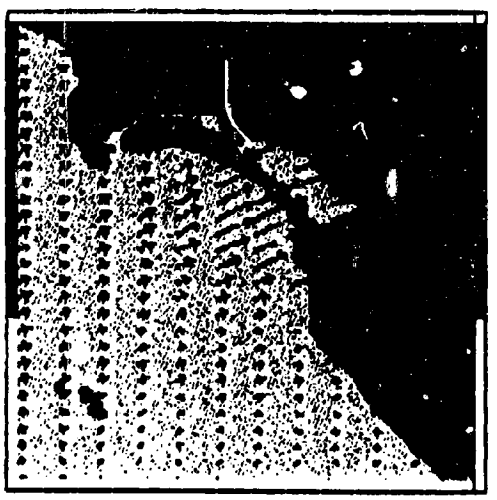

Wind Stress

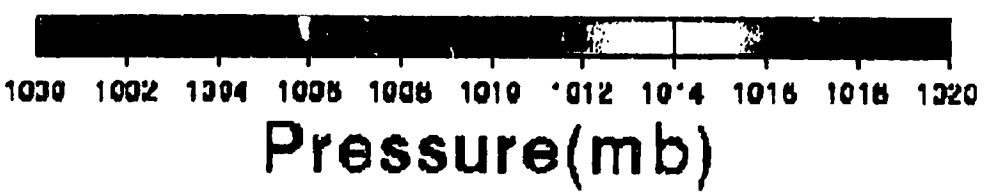

Figure 5

The second real-time case study was carried out in April 1996, in response to political turmoil in the West African nation of Liberia. Once again, the study was carried out at two different resolution in a nested fashion. The physical domain for the coarse grid stretched from the equator to 15° North and from 5° to 20° West. The area of interest included the cities of Monrovia (Liberia), Freetown (Sierra Leone), and the entire Liberian coast. At a resolution of 1/5 of a degree, the model was run on 76 by 76 grid points. The boundary conditions were setup using the database of global results available via the GUI. In all, 35 tidal stations were found in this domain, but only 22 were retained. The others were excluded based on their location (protected harbors, etc). The bathymetry was also setup using the GUI and the ETOPO5 database. The barotropic (external) time step was chosen as 30 seconds and the model was run with and without wind forcing. Time series plots for a station near Monrovia are shown in Figure 6. Figure 7 shows sample streak plots for the resultant barotropic currents with wind forcing for the coarse grid domain. The high resolution nested grid extended from 5° to 8.4° North and 8.7° to 13.2° West. The grid resolution was four times finer than the coarse grid or 1/20 of a degree. The selected domain yielded a 89 by 69 grid with two open boundaries (West and South). The boundary conditions were provided from the saved output of the coarse model run at the open boundaries of the nested domain. Data from only two tidal gages was available which was assimilated similarly. The barotropic time step was reduced to 8 seconds. A refined coastline and an accurate high resolution bathymetry was used. A sample streak plot and time series for Monrovia are shown in Figures 8 and 9 respectively. As before, fine resolution results capture greater detail and variability than the coarse resolution results.

FUTURE RESEARCH:

In building on our FY95-96 accomplishments, future plans include:

Task 1: Validation of the 2D model with Currents. The fully integrated 2D model has already been validated against tidal station data and sea level observations, and only the barotropic currents need to be validated. The barotropic influences weigh heavily in the coastal and shallow waters. The model predictions will be validated with any available observations in a suitable area.

Task 2: Application, Validation, and Integration of 3-D Baroclinic Model. Continue the applications and validation of the 3-D baroclinic model developed at CU under ONR sponsorship. This is a sigma-coordinate based, comprehensive physics 3-D tidal model (with data assimilation) used to provide estimates of tidal current structure (both vertical and horizontal) in coastal, marginal, and semi-enclosed seas. The model is currently running in the Yellow Sea at NRL, the Persian Gulf at NAVOCEANO, and is being configured for the South China Sea at CAST.

Prototype Tidal Model Elevation & Depth Averaged Currents with Surface Wind Forcing

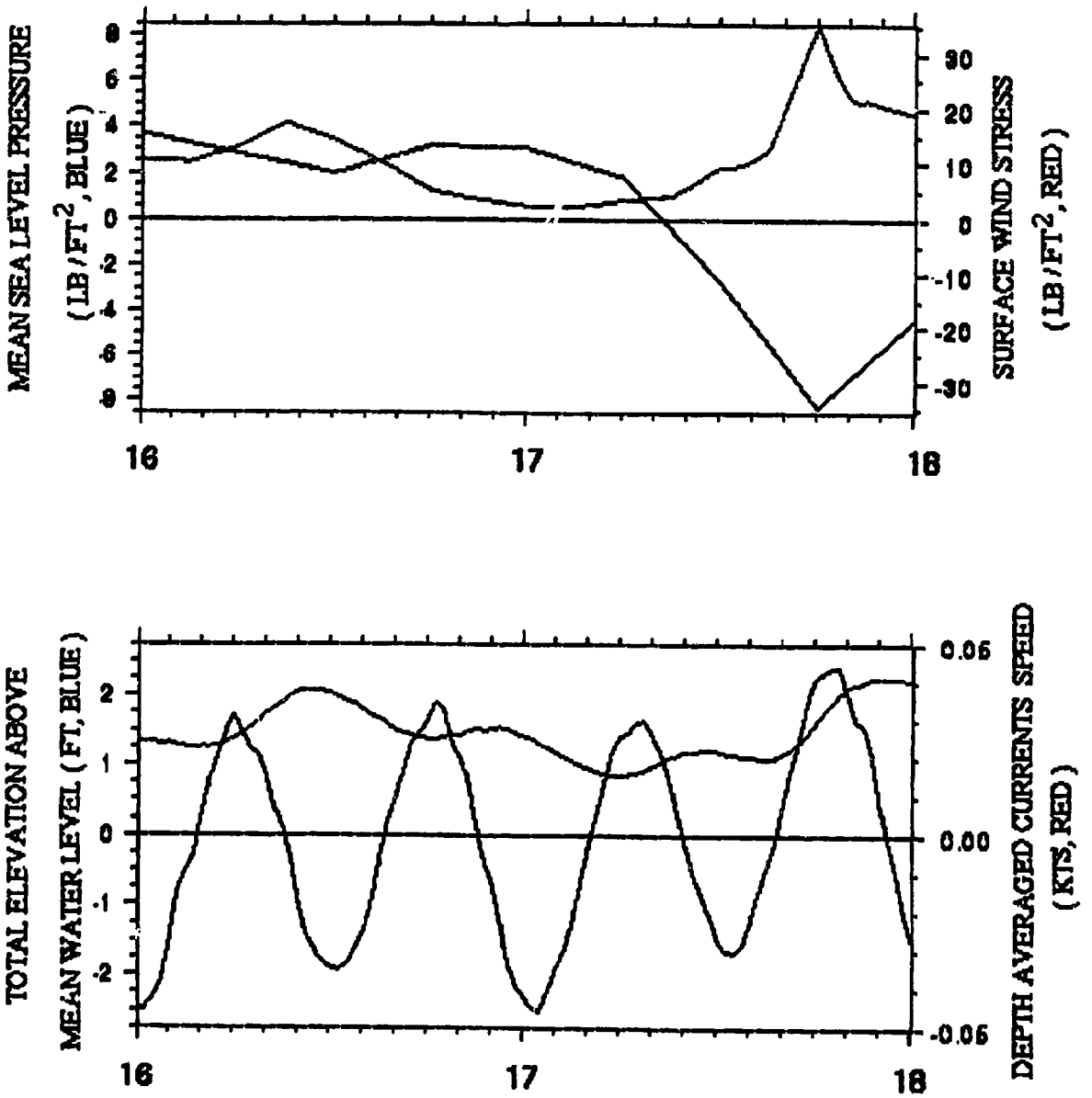

Figure 6. Time Series plots for Monrovia (Coarse Grid)

CURRENTSS Model

[Surface Winds Forcing]

Date = 17 Apr96 00 Hr

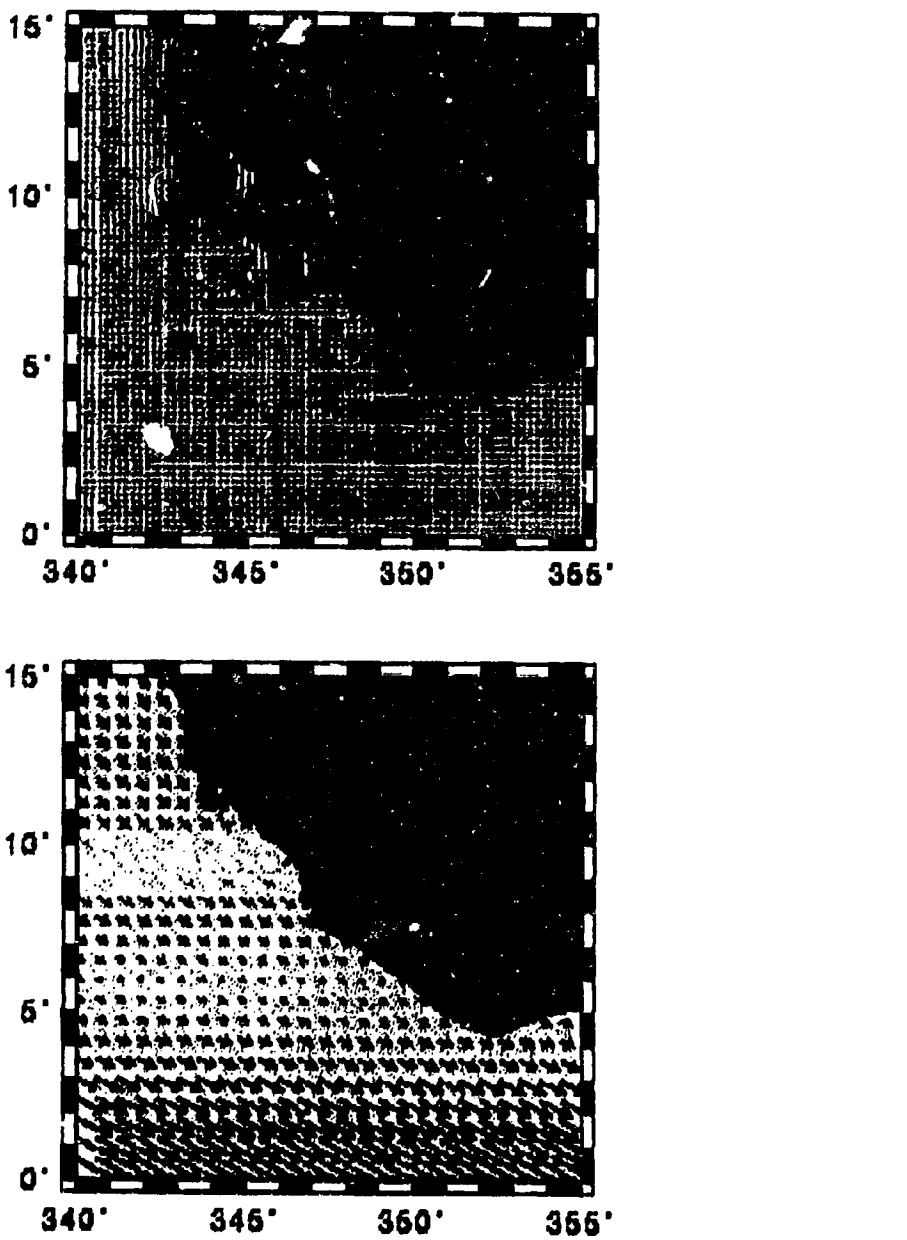

Figure 7. Streak-Plot of Tidal Currents for Coarse Grid Domain

CURRENTSS Model

[Surface Winds Forcing]

Date = 17 Apr96 00 Hr

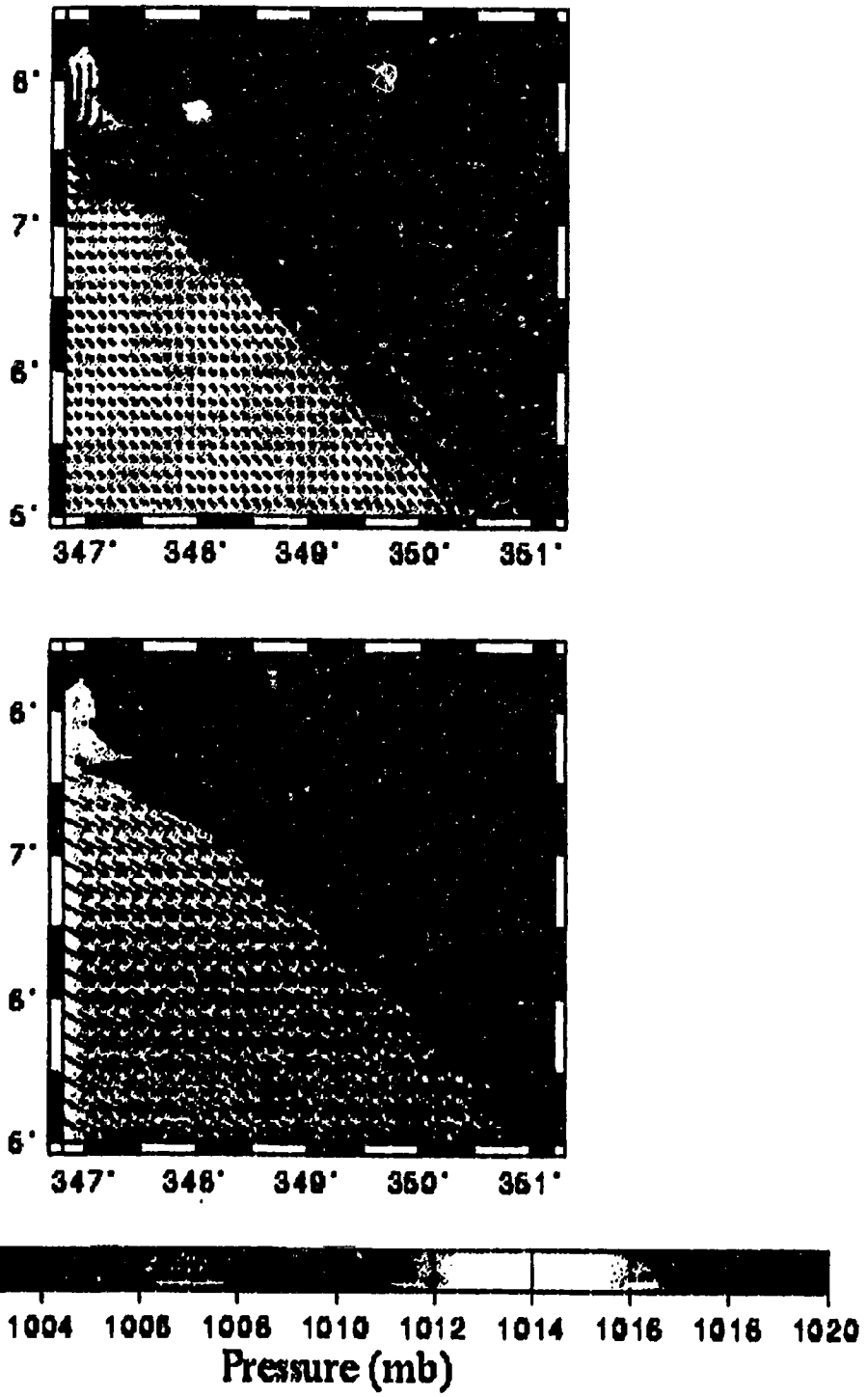

Figure 8. Streak-Plot of Tidal Currents for Fine Grid Domain

Prototype Tidal Model Elevation & Depth Averaged Currents with Surface Wind Forcing

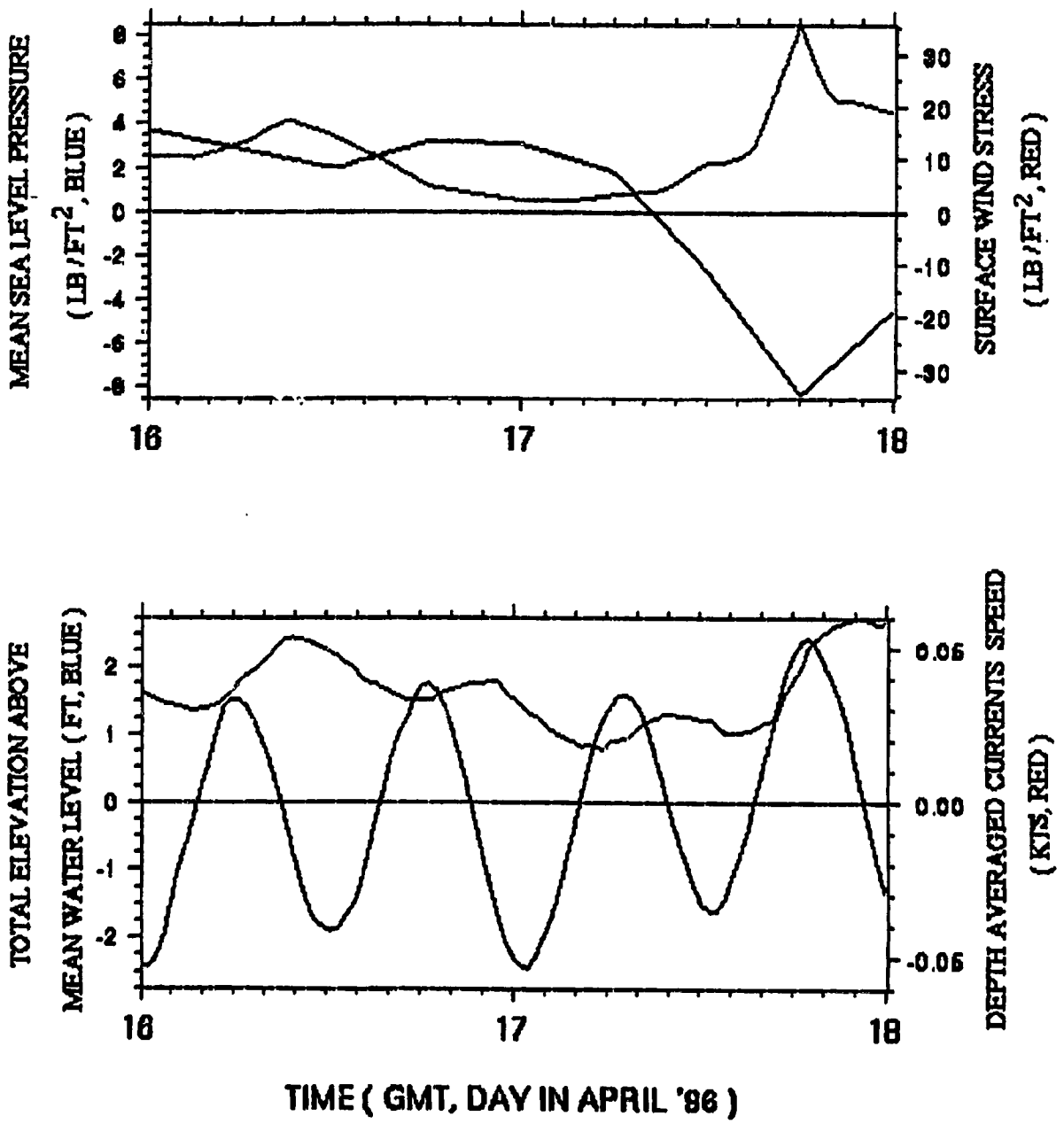

Figure 9. Time Series plots for Monrovia (Fine Grid)

Tidal currents are important in many applications including interpreting ADCP observations. While high resolution is preferable, because of the smaller scales involved (compared to tidal SSH), most often the data needed for initialization and forcing of high resolution tidal models are limited. There is also a need to nest high resolution tidal current models of the near coast to basin-wide coarse resolution models to provide the needed boundary conditions. It is with these in mind that CU will develop a 3-D tidal current model based on the same approach as the 2-D tidal SSH model, namely data assimilation to force realism and relocatable-nestable capability. The model will be applied to coastal, semi-enclosed, and marginal seas of Navy interest. MSU will build the GUI. The RME will be enhanced to support sigma coordinates and boundary conditions in the vertical. If reliable transport estimates are available they will be prescribed. If not, a mean geostrophic flow will be used. The model will be validated with current meter observations where available, and nested high resolution studies would be conducted if suitable data are available.

Task 3: Validation and Comparison of ADCIRC Model. NAVOCEANO's ADCIRC Finite Element Model output will be integrated into the RME for the purposes of model evaluation and comparison against available observational data and other appropriate criteria. Validation and inter-model comparison between the CU model and ADCIRC will be performed in close collaboration with NAVOCEANO and as such, will be conducted in earmarked regions of interest and with suitable parameterization developed in collaboration with NAVOCEANO. General guidelines will also be developed for the above, which will then be incorporated into the RME interface for the future validation of other relocatable models.

OTHER RESEARCH INTEREST: MODELING WITH DATA ASSIMILATION IN THE NORTH ATLANTIC (DAMEE)
by Dr. Avichal Mehra

SCIENTIFIC ADVISOR: Dr. David E. Dietrich

OBJECTIVE:

To show the strengths and weaknesses of different modeling/assimilation approaches.

APPROACH:

For the past two years, DAMEE-NAB has addressed the climatological behavior of different prognostic circulation models as per a fixed list of well documented properties of the North Atlantic Basin. Some forecast experiments on the target domain of the North Atlantic Subtropical Gyre have also been performed. These experiments entailed various data assimilation methods and emphasized synoptic time-scale predictions. All such experiments have been performed at a low resolution of 1/2° with fewer than 20 vertical levels. Future participants of DAMEE-NAB will address the sensitivity of mesoscale forecasts to variations in climatological measures, and also establish basin-scale predictive capabilities of general circulation models relative to persistence and climatology at higher resolutions (~1/10°) horizontally and a larger number of vertical levels (up to 40). Some other goals include identifying the strengths and weaknesses of different classes of numerical models and various data assimilation techniques. Exploring and implementing the best data assimilation methods with coupled models will be the final step for accurate, efficient forecasts of the North Atlantic Basin.

Recently DieCAST, with a modified Arakawa "a" grid scheme, was successfully implemented in the North Atlantic Basin at one-half degree resolution with ten vertical levels. The domain extended from 15°S to 65°N, and from the equator to 80°W. It included the entire North Atlantic basin and Atlantic Equatorial Region, but excluded the Gulf of Mexico. The vertical viscosity was determined by a method based on Richardson number, while realistically low horizontal diffusivities were specified to model the circulation. Results indicate active inertial eddy fields caused by implementation of higher-order interpolations and modifying the incompressibility algorithm to substantially reduce dispersion. Even at a coarse resolution of one-half degree, the Gulf-Stream separation seems robust (see Figure 10) and other well-known features of the North Atlantic Subtropical Gyre were reasonably simulated. Particularly striking are realistic

Figure 10

detailed features associated with the Flemish Cap (Figure 10). This includes an anticyclonic Taylor column; an anticyclonic Gulf Stream water penetration east of the Flemish cap into the Labrador Sea, between two semipermanent small-scale cyclonic features; and a southward moving central Labrador Current branch in the Flemish Channel on the west side of the Flemish Cap, with the full observed three branch system clearly shown in the Labrador Sea. This research involves the following three tasks.

1. Comparison with Observations. DieCAST will be implemented at 1/10° resolution with 40 z-levels in the North Atlantic Basin including the Gulf of Mexico. As noted above, reasonable results have already been obtained using 1/2° resolution and 10 z-levels. To be sure that the model is converged, an intermediate resolution run will also be performed. The NAVOCEANO GDEM climatology will be used along with ECMWF (1993) winds with variability. Some results that will be analyzed include the mean and seasonal cycle of Florida Straits water at 27.5°N, eddy kinetic energy distributions at various depths, mean and variance of Gulf-stream path, and separation at Cape Hatteras. Certain model vertical cross-sections at 27°N and 55°W will also be compared and contrasted against observations. Model outputs adequate to show performance criteria will be included. In addition, because transient eddies may be critical to the maintenance of the Labrador Current between the Grand Banks and Cape Hatteras and thus also to the realistic GS separation, diagnostics to assess the roles of transient eddies ("negative viscosity" alias "Neptune effect") will be included.

2. Study Thermohaline Circulation. The Labrador Sea is one of the most intensive water mass transformation regions of the world. It affects the thermohaline circulation of the entire NAB. In the DAMEE experiment, this is treated through specification of a northern buffer zone climatology to obtain proper deep water inflows from the Labrador Sea. To model the water mass transformations more directly, the domain may have to be extended to 75°N (if resources allow). The resulting thermohaline effects will be addressed by (a) exploring the sensitivity of the circulation to turbulent vertical diffusion, downward diffusion of latitudinally differential density from surface heat and salinity fluxes creates available potential energy for the thermohaline circulation; (b) maintaining a diagnostic time mean of model surface heat and salinity fluxes at all horizontal grid points; (c) adding the long term mean model heat and salinity heat fluxes to the surface layer each time step; (d) after adding the long term mean fluxes, restoring to GDEM with O (180) day restoring time scale each step; and (e) using the streamfunction for the zonally averaged flow to diagnose thermohaline effects on the meridional circulation

3. Implement Data Assimilation. The DieCAST ocean model capabilities will be enhanced by incorporating the best/most practicable data assimilation.

OTHER RESEARCH INTEREST: A NESTED HYBRID MODELING SYSTEM
by Dr. Avichal Mehra

OBJECTIVE:

To deliver an accurate and efficient hybrid modeling system for nowcast/forecast applications for ocean/tidal currents and sea surface height.

APPROACH:

DieCAST is an efficient, robust, accurate model in application to deep water and to coupled coastal flows, as well as to island wakes and detailed high resolution flows in a fjord. These positive attributes result from its rigid-lid approximation, z-level vertical coordinate, conservative control volume numerics, and special accurate treatment of Coriolis and internal wave propagation terms. A free surface with explicit time-split barotropic mode has been recently added.

CURReNTSS is a sigma coordinate, finite difference, explicit, vertically-integrated barotropic model assimilating tidal data from coastal gages and from bottom pressure gages. It is fully non-linear and incorporates direct astronomical forcing, and can also include surface forcing from atmospheric models to predict storm surges. The model can be run with any number of components including long term and compound tides. It employs a simple data assimilation procedure by replacing the model predicted SSH at pre-determined intervals by a weighted sum of the model prediction and the observed SSH from the tide/bottom pressure at that point, the weights determined a priori. The model is well formulated, carefully calibrated and adequately validated for a number of regions. The basic problem is that while bottom boundary fit approaches (such as sigma coordinates) may be attractive for very shallow regions, they are not designed for accurate representation of baroclinic pressure gradient and vortex stretching terms, which involve gradients of density and horizontal velocity in regions of large amplitude and steep topography.

Dr. Paul Martin (NRL) has noted the stair-step approximation can cause spurious local horizontal divergence that does not occur in sigma coordinate models. He also noted that when the pycnocline appears as a sharp "horizontal" front because of sloping sigma surfaces, horizontal advection errors can be amplified. This can lead to large spurious oscillations when using realistic diffusivities. However, large diffusivities are undesirable because they can cause unrealistic cross-pycnocline mixing. In z-level models, horizontal advection errors are smaller, because the pycnocline is quasi-horizontal and thus easier to

resolve horizontally, while vertical advection errors are small simply because buoyancy suppresses vertical velocity properly near thermoclines in z-level models. It thus seems appropriate to blend sigma coordinate coastal models with deep water models. This is presently being done by Dr. D.S. Ko in coupling the Princeton Model to the Navy Layered Model and by Dr. Martin within a single model. DieCAST provides another option, because it can be used with the high vertical resolution needed for accurate coastal modeling and can conveniently address air-sea exchanges. The goal is to use DieCAST to provide deep water open boundary conditions to the coastal model and/or use the models as a fully coupled system. Tasks involved are:

1. Blend of sigma and z-level co-ordinates. Techniques to modify sigma coordinate surfaces instead of the often used topographic filter approach will be investigated to improve pressure gradient and vortex stretching numerics. Such modifications reduce vertical coordinate surface slopes in deep water, without affecting bottom topography. This may avoid the need for topographic filters. Two approaches will be considered. The first approach (filters) will start with conventional sigma coordinate surfaces. These will be filtered by iterative application of a Laplacian filter designed to decrease large coordinate surface slopes, but only when they are away from the bottom; the slope damping will be proportional to the distance from the bottom. The second approach is to define each individual vertical coordinate surface as a function of depth such that it is quasi-horizontal in areas deeper than a specified depth. Thus, its depth function will asymptotically approach a specified value as the depth increases. The resulting vertical surfaces will substantially deviate from sigma coordinates, but little or no change will be needed to use their metrics in conventional sigma coordinate models.

2. Flux conserving nesting. The first requirement by a nested submodel is the normal boundary velocity, which must have integrated zero volume flux. The other fundamental boundary quantities that must be conserved are momentum, salinity and heat fluxes. It may be simplest and best to specify the actual nested fluxes of momentum, salinity and heat from the z-level coarse model. This eliminates guess work for open boundary flux specification and allows a consistent interior nested domain solution to develop. Initially, the coupling will be implemented between the Arakawa "c" grid version of DieCAST and CURReNTS. Later, the Arakawa "a" grid version will be used. Such a hybrid system would take advantage of the strong features of both z and sigma level modeling techniques. It would provide less dispersive, more accurate and efficient results for deep water, and their use for accurate predictions for coastal currents, tides and sea surface elevations from sigma-level model.

A STUDY OF EDDY DYNAMICS IN THE NAVY LAYERED PACIFIC OCEAN MODEL DATA

by Dr. Zhifan Zhu

SCIENTIFIC ADVISOR: Dr. Robert Moorhead, MSU-NSF Engineering Research Center

OBJECTIVE:

Eddies are prominent ocean features and play a critical role in ocean circulation modeling and prediction.They are time-dependent oceanic phenomena that exist ubiquitously in ocean circulations and are often associated with strong barometric and thermal variabilities such as low/high pressure centers and radial temperature gradients. Various interactions and coupling effects between mesoscale eddies, ocean currents, and heat transport have long been studied. However, due to the complex mechanisms involved in eddy dynamics, many eddy aspects are not understood; how eddies contribute to and interact with the dynamics of other oceanic features remains largely unresolved. Characterizing eddy dynamics over time and space has thus been of keen interest to physical oceanographers in recent decades and continues to be a major research topic in physical oceanography

Modeling of global scale ocean circulations has recently become an important means of oceanographic studies. In particular, models with eddy-resolving capability, have played a central role in global ocean prediction. The time-varying three-dimensional model outputs consist of high resolution data samples of the ocean circulation fields and are well suited to the study of eddy dynamics. Here the objective was to conduct an investigation of eddies in two regions of the Navy Layered Pacific Model data from 1983 to 1987.

APPROACH:

The approach is based on an eddy extraction algorithm developed for extracting and visualizing eddies from time-dependent flow fields. The Navy Layered Ocean Model was developed by the Naval Research Laboratories (NRL) at Stennis Space Center. The data used was from a 1/6° eddy-resolving model of the Pacific Ocean north of 20°S. Artificial solid boundaries are placed at 20°S and in the straits at the southern boundary of the Indonesian Archipelago. Horizontally, the model covers the area from 110°E to 78°W and from 20°S to 62°N, with a horizontal resolution of 0.125° x 0.176° (lat, lon) for each variable. Vertically, it has 6 layers with mean interface depths of 135, 320, 550, 800, and 1050 meters. The other major features of the model include nonlinear primitive equations, a free surface, a semi-implicit time scheme, full-scale bottom topography in the lowest layer, and an arbitrary coastline geometry.

Starting from rest, the model was spun up to statistical equilibrium at 1/4° resolution using the Hellerman-Rosenstein monthly wind-stress climatology, and then continued another 15 years at 1/8° resolution. Finally, it was run for 1981-1989 using monthly averaged ECMWF 1000-mb winds with the 1981-1989 mean replaced by the annual mean from Hellerman-Rosenstein. No oceanic data were assimilated in this purely wind-forced simulation. Verification of the model was conducted using satellite altimeter data from the Geosat Exact Repeat Mission (ERM). Dr. James Mitchell (NRL) compared the statistics of the simulated and observed SSH variations for the Kuroshio Extension; while Gregg Jacobs (NRL) analyzed the two SSH variabilities through frequency-wavenumber decomposition. Both studies reported good correlation between model and altimeter SSH variations.

The output consists of layer thickness deviation 'H' and horizontal transport velocity $\{\vec{V} = (U,V)\}$ for a 3.05 model day interval at each layer and horizontal location. The relationship of flow velocity $\vec{v}_k$ and transport velocity $\vec{V}_k$ at the kth layer is given by:

$$\vec{V}_k = h_k \vec{v}_k$$

where h_k is the layer thickness which can be derived from H_k and the reference depth. The total data size for a four-year run is about 22 gigabytes.

Two regions were selected for the study. Region A is from 110°W to 145°W and from 15°N to 62°N along the west coast of North America, and Region B extends from 120°E to 180°E and from 20°N to 55°N, containing the Kuroshio Current near Japan.

The algorithm extracts eddies from the time-varying volumetric flow fields and stores them in an abstract form. Each extracted eddy consists of a sequence of eddy instances (in a 3D spatial sense) from emergence to decay. Each instance is further decomposed into a stack of horizontal slices (2D layers). The number of slices can vary from one to six. A minimum life-span threshold was imposed in this calculation; eddies that existed less than two months were excluded.

RESULTS:

Given a two-month life time criterion, 207 eddies in Region A and 314 eddies in Region B were extracted from the four year data. The most persistent eddy in Region A had a life-span of 311.1 days while in Region B it was 741.2 days. These 521 eddies form the basis of the following analysis.

a. Trajectories. Figures 1a and 1b show the eddy trajectories visualized by tracing the centers of the tracked eddies. The red represents cyclonic eddies and the yellow anticyclonic eddies. The grayish background is the bathymetry. Notice that the images show the superimposing eddy migration paths during the four year period. The time information is lacking. This information can be effectively investigated by an interactive animation process, which is not permitted here.

The eddies in Region A are concentrated off the California Coast with the densest areas below 40°N. While below 30°N the eddy's movements are consistently in the horizontal direction, the eddies from 30°N to 40 N near the coast moved in multiple directions. Long migration paths are easily seen away from the coast below 30°N. These eddies were created from the water flowing parallel to the North Equatorial Current. The existence of alternating cyclonic and anticyclonic eddies from 15°N to 35°N (west of 130°W) suggests significant horizontal currents in that area, causing the eddies to be pinched off above and below the currents. The eddies at the high latitudes (above 40°N) were mostly anticyclonic, which tend to meander in the littoral waters. No (long-term) eddies were found above 35°N.

The average migration distance of the eddies in Region A is 454.46 kms and the mean speed is 5.07 cms/s. In general, the eddies at the lower latitudes showed larger speeds. The speed difference between the cyclonic and the anticyclonic eddies is trivial, although there were twice as many cyclonic as anticyclonic eddies.

Region B can be divided into three separate areas: Sea of Japan, Sea of Okhotsk, and the NW Pacific region. Since higher resolution models of the Sea of Japan exist, and the Sea of Okhotsk is only partially covered, the analysis here is focused on the Pacific region which includes the Kuroshio Extension. The eddy trajectories are in an elongated area around the Kuroshio Current. The number of cyclonic and anticyclonic eddies is almost equal. The highest eddy density occurred in the area to the west of the Shatsky Rise and extended northeastward to the Emperor Seamount Chain (at ~170°E). The trajectories are non-linear, revealing the great energy and complexity of currents surrounding the Kursohio Extension. Beyond the Emperor Seamount Chain, most eddies wandered in small areas creating twisted trajectories. Most of the coastal eddies can be found off the Tsugaru Strait. The tangled lines show the superimposing eddy trajectories over the four years. The long and stretched pathlines are a distinct pattern in the western part of the Kuroshio (below ~31°N), particularly across the Izu Ridge. These eddies were created from rings pinched off the horizontal stream. The average distance of eddy migration in this region is 434.50 kms, and the average speed is 4.80 cms/s. Noteworthy is that Aoki reported a typical speed of 4 cm/s for two strong cyclonic eddies tracked in the first year (from November 1986 to November 1987) Geosat ERM altimeter data around the Kuroshio Extension.

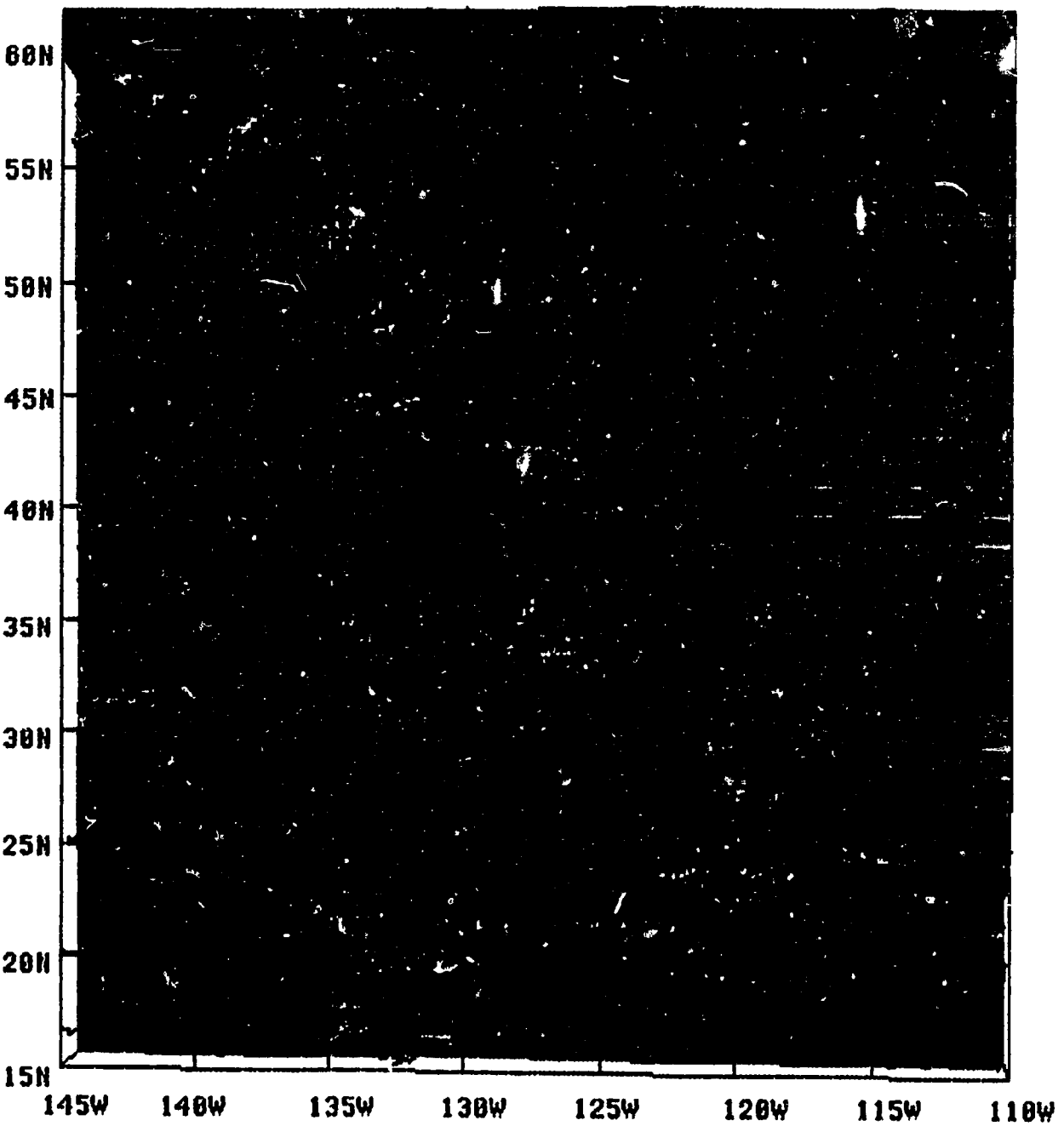

Figure 1a. Region A.

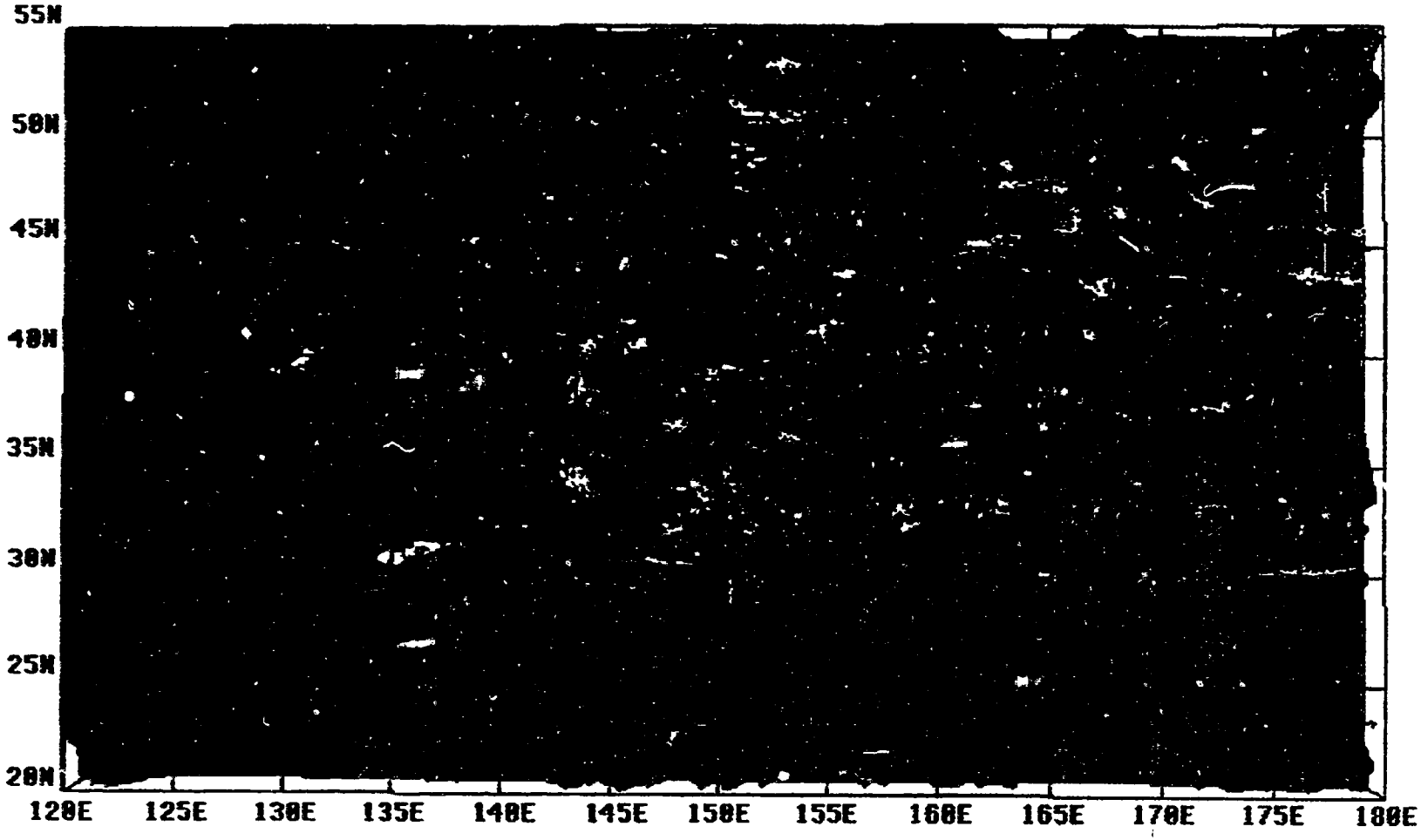

Figure 1b. Region B.

b. Time sequences of eddy densities. It is known that eddies carry significant amounts of energy in various interactions with the oceanic and atmospheric fields. The eddy field has a direct influence on the global heat budget and surface and subsurface variabilities, and vice versa. Such a relationship can be examined by observing the density of the eddy fields over time. The density of the eddy field is represented by the number of eddies that exist at a particular time. In Figure 2 are two curves showing the results for each model day during the four years. The eddy field in Region B is generally correlated with the season, e.g., more eddies exist in the summer time than during the winter. The annual peaks are around August-September. A small peak in January 1985 indicates an 'anomaly'. The variations are generally in agreement with the seasonal cycle as estimated by Tai and White (1990) using the rms sea level variability from GEOSAT. Since the eddy field around the Kuroshio Extension is primarily forced by the instabilities of the strong current, one would expect a similar cycle in the current. The eddy field in Region A shows a seasonal correlation only in the last two years (1985-86). In particular, a sudden drop in eddy density occurred in the summer of 1983 and caused an 180° out of phase until the spring of 1985. This phenomenon may be related to the strong El Niño event ending in 1983, the fact that low latitude variability is less seasonal by itself (Pond and Richard, 1983), and the fact that the amount of vertical motion in the littoral areas may mask the seasonality.

The auto-correlation functions of the two time sequences in Figure 2 are shown in Figure 3. The alternating pattern for Region B is a strong indication of the eddy field varying in seasonal cycles.

c. Sea surface height (SSH) of eddy centers. The SSHs are computed at the top-layer eddy centers, and are averaged separately over the cyclonic and anticyclonic eddies at each time step. They indicate the variability of the sea surface elevation of the eddy field. Figure 4 shows the variations of SSHs over time. In Region A, the SSHs of the cyclonic eddies and anticyclonic eddies vary in similar patterns over time, indicating that the SSHs of the eddy field closely follow the overall SSHs in the domain. This is probably because the amplitude of sea surface variations at the eddy centers caused by the vertical water transportation is only a fraction of the domain SSH deviations. In Region B, the correlations between the cyclonic and anticyclonic SSH patterns are not as obvious as in Region A, and the magnitude of the SSH variations is about twice as large as that in Region A, thus indicating the model output being consistent with climatology because eddies are more energetic towards the west in the North Pacific Ocean.

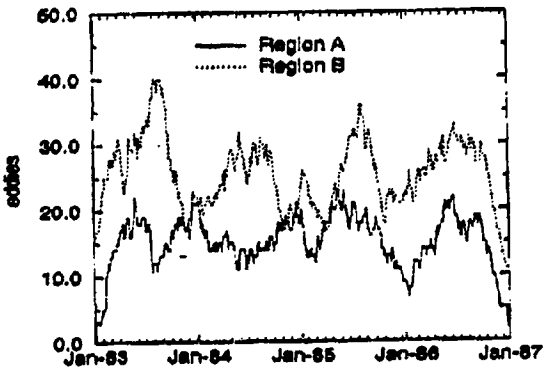

Figure 2. Time sequences of the number of tracked eddies.

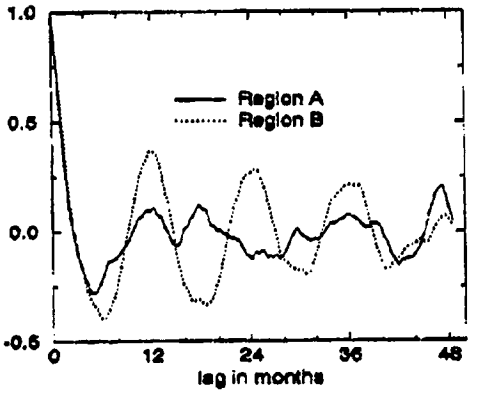

Figure 3. Auto-correlation function of the time sequences of the number of tracked eddies.

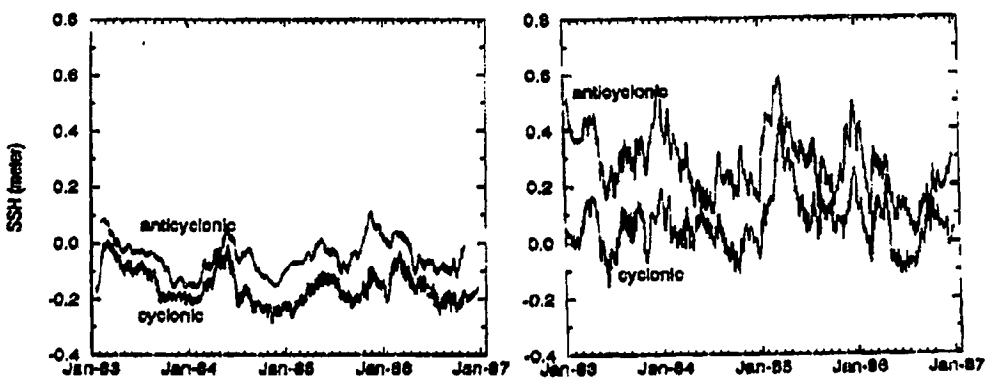

a. Region A

b. Region B

Figure 4. Sea-surface height at the eddy centers.

FUTURE RESEARCH:

Future efforts will be directed at creating a system that can intelligently digest large amount of raw data and save the most relevant information as features in an object-oriented database for various oceanographic applications. The system should be able to provide a high-level description of ocean physics at a given time and place. Such information, based on the features stored in the database, should be sufficient for a user to characterize the physical domain under study.

ENVIRONMENTAL DATA VISUALIZATION SYSTEM VERSION 2.0 (ENVIS 2.0)

by Dr. Zhifan Zhu

SCIENTIFIC ADVISOR: Dr. Harsh Anand, Center for Air Sea Technology

TECHNICAL ADVISOR: Mr. James Corbin, Center for Air Sea Technology

OBJECTIVE:

The development of ENVIS 2.0 is based on ENVIS 1.0 and the Unified Air Sea Visualization System (UASVS). ENVIS was developed as a tool that emphasized feature detection capabilities, and it received positive feedback from oceanographic data visualization applications. However, the software was built upon Silicon Graphics workstations and its data interface capability was limited. UASVS focused on the gridding structures present in different ocean model data sets. It allows one to map the original grids to a single, unified grid so users can easily visualize and compare the results of various models. Although both ENVIS and UASVS possess attractive functionalities, their non-objected-oriented nature makes them difficult to upgrade.

The objective of ENVIS 2.0 is to incorporate, refine and expand the data visualization capabilities of ENVIS 1.0 and UASVS, using object-oriented designs. That will provide flexibility in maintaining and updating the system. The immediate improvements include simultaneously visualizing time-varying 3D data objects with different time and spatial scales, without interpolating data, i.e., data objects will be kept in their original resolutions and formats; interactive edition of graphic object attributes, e.g., individual colormap and texture will be associated with each graphic object; interactive edition of text labels, i.e., allowing the user to generate and edit text labels in the fly; animation of graphic objects in time and space and the time-space animation information can be saved and loaded for successive rendering; and allowing output to rendered images in various formats to generate postscript visual presentation. The ultimate goal of ENVIS is to make it a scalable visualization structure such that various applications can be built effectively and efficiently. Applications may include stand-alone visualization tools on different platforms, and functional modules integrated in a distributed modeling and data management environment using CORBA/EDGE technology currently being developed at CAST.

APPROACH:

In order to achieve interoperability and portability using object-oriented techniques, the essential functionalities of ENVIS 2.0 are grouped into hierarchies

of classes. These hierarchies include data object, graphic object, render class, GUI, animation, image, and label classes. Since we are dealing with heterogeneous data sources (e.g., grids and formats), a data class hierarchy needs to be developed. The root class is an abstract class under which specific data interface classes are created. These data classes have unified API with other class groups and are able to handle various data sources implicitly.

The graphic object classes consist of polygons, mapping routines to map the data objects into graphic objects, and rendering routines. These routines are primarily written in OpenGL, a predominant graphic language supported by most graphic workstations. Render classes consist of a pool of machine dependent renders. First, the rendering classes are designed for each type of machine, e.g., SGIs and SUNs. Then sub-classes are developed with each parent class. For SGIs, the sub-classes will be based on their graphic hardware capabilities, e.g., Indy 8-bit, Indy 24-bit, Indigo2 Extreme, Indigo2 High Impact, etc., to assure an economical fit. Under the same hardware render class, 2D and 3D render classes are created for different applications.

The development of GUI classes is not a major task in ENVIS 2.0. The effort is leveraged with other projects at CAST to create a unified GUI library. In particular, ENVIS 2.0 can be integrated as a visualization model in an application, such as Weather Watch. No top level GUI is needed. Animation, image, and label classes are supporting classes to facilitate the rendering process and creation of technical presentations.

RESULTS:

A prototype of ENVIS 2.0 has been developed. It consists of libraries of classes grouped in functional hierarchies. Additions of new classes within a class hierarchy do not affect the interface with other class hierarchies. Figure 5 displays the relationship among these class hierarchies.

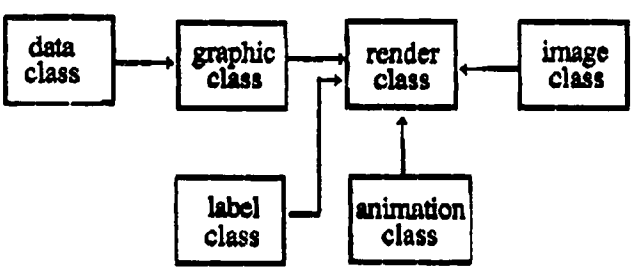

Figure 5. Class relationships.

Corresponding GUIs have been developed to integrate these functional objects into a visualization tool that the user can steer. Figure 6 shows ENVIS 2.0 GUIs which are implemented with a Motif class library. The mainwindow contains a SGI render and toplevel menu bar to launch other GUIs. DataManager lets the user manage data objects, e.g., loading and deleting. It also allows selection of section of data from a data object for mapping. ViewManager controls the mapped graphic objects, e.g., selecting or deselecting graphic objects, or modifying the graphic attributes such as colormap and opacity of selected graphic objects. GraphicAttr maintains a workspace to allow the user to modify graphic attributes. LabelManager controls the creation, deletion and modification of label objects such as string labels, time information display, and colorbars. ImageManager allows one to save currently rendered images in any supported image formats. AnimateManager provides controls of the animation in both time and space. For temporal animation, the user can select any time window and time increment to animate the timed graphic objects in both forward and backward directions. For space animation, the user can pre-register viewing angles and positions interactively and play back. The time and space animation can be used simultaneously. Animation information, such as time stamps and viewing angles, can be saved to and loaded from a simple text file for session recording.

Figure 6. Snapshot of ENVIS 2.0 GUIs.

The Figure 7 shows an example of using Envis 2.0 to visualize Persian Gulf temperature and current fields from the Princeton Ocean Model. This version of the model has a horizontal curvilinear and vertical sigma gridding structure. The temperature is visualized by color-fill contours with the color map displayed on the right side of the image. The current is rendered by streamlines superimposed on the temperature field. The terrain and bathymetry are shown in a different color map. All the rendered graphics are treated as graphic objects. They can be 'turned on and off' by selecting and deselecting their icons in the GUI. Their graphic attributes can be interactively modified. For example, the temperature color contours and the terrain-bathymetry have their own color maps to enhance the visual effectiveness. The 3D graphic objects can be easily transformed (translated, rotated, and zoomed in and out) with the mouse. The labels (including the color map) can be picked and placed at any location in the window. Their fonts can be altered interactively.

Because of the object-oriented data class design, different types of data grids and formats can be easily supported and visualized in the same volume of time-space. There is no centralized gridding system. Data objects are mapped into graphic objects directly from their original grids and resolutions. This greatly reduces the cost of copying and re-formating data.

FUTURE RESEARCH:

Further efforts in developing ENVIS will be focused on developing and integrating function classes to be portable across many display environments. To do so, a common interface approach will be adopted. This effort will be performed in conjunction with the Extensible Dynamic GUI Environment (EDGE), a research effort currently conducted by CAST. With this technique, ENVIS 2.0 visualization capability will be easily integrated into any modeling and information management system operating on most, if not all, platforms.

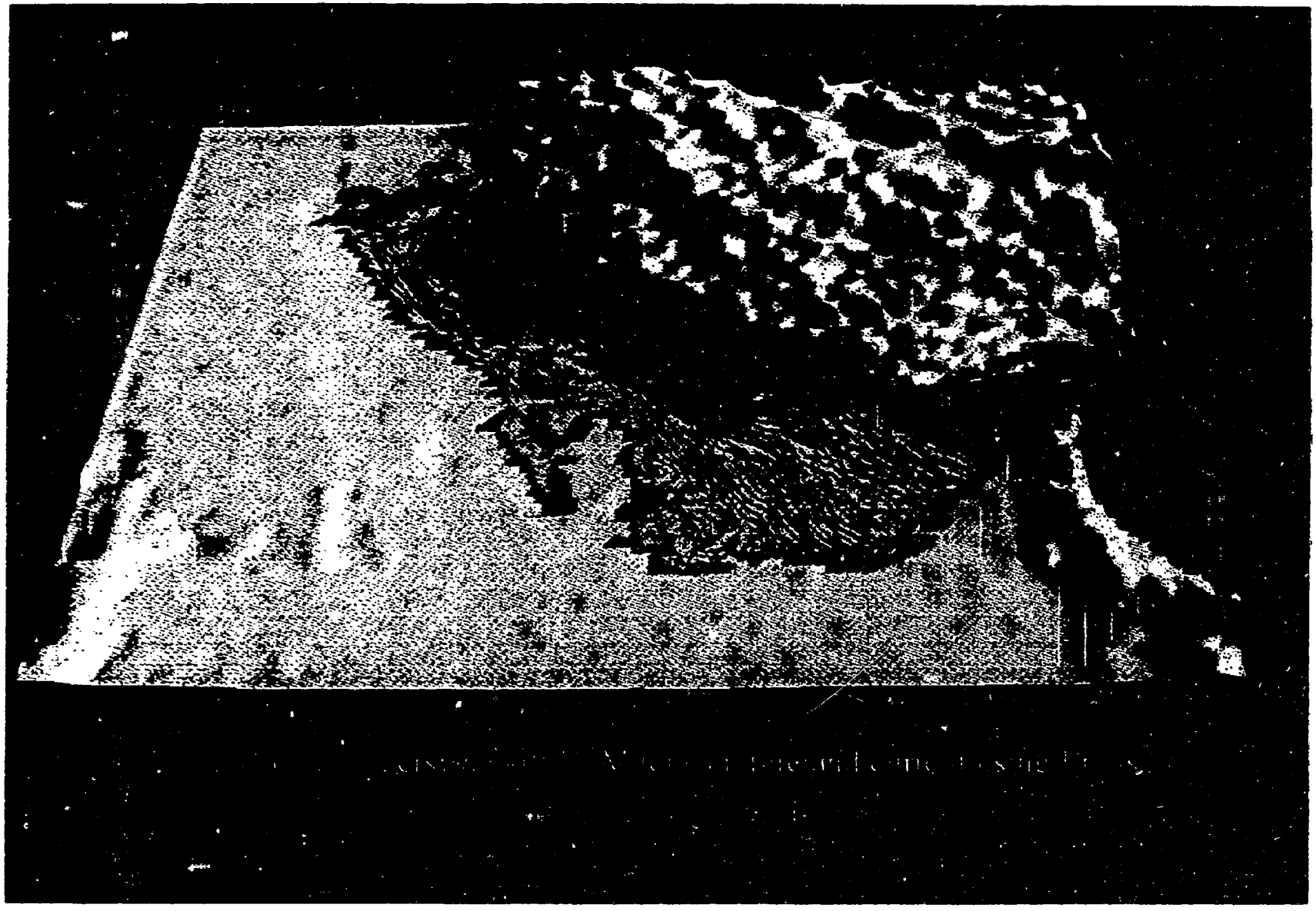

Figure 7. Visualization of Persian Gulf POM temperature and current using

OTHER RESEARCH INTEREST: DISTRIBUTED MULTI-RESOLUTION VISUALIZATION

by Dr. Zhifan Zhu

OBJECTIVE:

Creating better models and obtaining more and better data has always been a challenge in ocean modeling and simulation. Perceiving, understanding, and communicating the knowledge contained in the model's output or the measured data is critical. The fundamental problem, as models get larger and computers get faster, is the need to examine and understand more data, in increasing detail but in the same amount of time. Distributed visualization provides collaboration, concurrentness, and computer/visualization resource efficiency. It is an important emerging technology that will enable scientific programmers to extract meaningful information rapidly from detailed simulations, by eliminating much of the disk-to-disk copying that is now performed.

A typical situation of a model-visualization configuration is that the model is running on a large and fast supercomputer or running in parallel over a cluster of networked computers. Parallel computation allows partition of a large model into a set of solvers each running on a single processor. The results will be collected in real-time and sent to a graphic workstation for visualization. The visualization is in fact a part of model steering that allows the modeler to interactively monitor the simulation by visualizing the results and controlling the simulation according to the visualized results. In this way, large amounts of data often need to be transferred from the solvers to the graphic workstation through the local area network and/or wide area network. To achieve real or near real-time operation, data traffic has to be minimized. This can be done with multi-resolution and data compression techniques. Multi-resolution means that the modeler can choose different resolutions in visualizing the model data. In particular, data will be transmitted in a way that visualization can begin at a lower resolution and be refined to higher resolution. The transmission can be stopped once sufficient information is visualized. It has been identified that the whole process involves multi-resolution data transform and compression. The objective of this research is to develop multi-resolution and data compression techniques that best suit the distributed visualization paradigm.

APPROACH:

The data transform plays two roles: packing the data in a multi-resolution form that can be progressively transferred, and decorrelating the original data points so the transformed data can be compressed at a higher compression ratio. Dependent on lossy or lossless criteria, compression can be implemented using

entropy coding or other technique. The research can be tasked in two aspects: transform and compression techniques.

Wavelet transform has recently been found to be a powerful tool in signal processing, and in multi-resolution analysis in particular. For multi-resolution applications, wavelet transform filters the data into a set of bands that correspond to different levels of details. The transformed data are then transmitted in bands from lower to higher resolution, and a perfect reconstruction of the original data can be achieved with all the data bands. The issues involved include selection of good wavelet filters, optimization of block partition, and integer/reversible transform.

For multi-resolution signal processing, wavelet transform serves as a digital filter with compact support. The aim here is to have a filter that can maximally pack the energy in a minimal number of coefficients, and be computationally less expensive. The efficient use of wavelet transforms requires that the dimensions of the data are the powers of certain integers. For fast data manipulation, the data dimension is required to be dyatic, i.e., power of 2. Unfortunately, in the real world, the data dimensions are quite arbitrary. Therefore data partition is often needed to divide the data into small blocks, e.g., 4 x 4 x 4 or 8 x 8 x 8. Data partition helps eliminate/reduce the overhead introduced by padding when treating the data volume as a single block. However, it also affects the efficiency of wavelet transform. For example, if the data is smooth, a large block size for wavelet transform will result in larger energy packed in a smaller number of coefficients. Therefore, to achieve good wavelet transform effects, data partition must be fine tuned.

The integer wavelet transform technique deals with lossless compression. General wavelet transform will create transform coefficients as floating numbers, no matter whether the original data are integer or floating. Lossless compression of floating number is difficult. In practice, a floating number is often separated by its exponent and mantissa and compressed separately. Since wavelet transform decorrelates the data to increase the signal entropy, this decorrelation may not be carried into the exponent and mantissa. Using integer wavelet transform on the exponent and mantissa integers of the original data may solve the problem at the cost of double wavelet transform computations. This extra computational load can be reduced by the integer operation of the integer wavelet transform.

Efficient compressing wavelet coefficients requires investigation of the entropy distributions. For entropy coding, multiple codebooks are suggested for different bands of coefficients. In addition, embedded coding techniques, which code bits instead of bytes, will be studied to explore multi-resolution.

OTHER RESEARCH INTEREST: TEXTURE MAPPING FOR FLOW VISUALIZATION
by Dr. Zhifan Zhu

OBJECTIVE:

Visualizing flow fields is a challenging task. Effective and realistic visualization requires a vivid display of both flow directions and amplitudes. Texture mapping is a technique used in computer graphics to map a texture pattern, often an image, to an object surface. The use of it to visualize numerical flow fields have been proposed. The idea is to create texture images that map the flow fields, and then animate the texture images. The mapped texture image contains pixel clusters (randomly positioned in the background) that are blurred and deformed in the flow directions, and are shaped by the flow amplitude to achieve a realistic visual effect. Such an image is repeatedly computed with a certain phase shift applied to the pixels in the flow directions to create a sequence of texture images for animation.

Two popular texture mapping techniques are Line Integral Convolution (LIC) and Spot Noise. The LIC method computes local streamlines for each pixel position of a random input image and determines the output pixel value by integration along the streamline. The Spot technique takes an input image consisting of random spots in the background and computes a local stream-surface for each spot, and then deforms the spots according to the local stream-surface. Since the Spot method uses 2-D deformation, flow amplitudes can be visualized via the varying width of the spot, but generally it is more computationally expensive than LIC. Both the LIC and the Spot algorithms have been used in computational fluid dynamics (CFD) applications to visualize surface flows near the objects in CFD fields.

APPROACH:

A frequency-modulation (FM) technique was used in computing the texture patterns modulated by the underlying flow field. The algorithm is mathematically straightforward and easily implemented. Similar to LIC, the FM approach is a 1-D operation along the streamline direction; however, it uses global instead of local streamlines, and convolution is replaced by frequency modulation. The technique is omputationally efficient and produces effective visualization. The FM signal can be mathematically written as:

$$y(t) = A\cos[\psi(\tau)] = A\cos[\omega\tau + X\theta(\tau) + \beta]$$

where A, ω, C, and β are the time-invariant parameters of the signal representing the amplitude, carrier frequency, modulation index, and a constant phase shift. The instantaneous frequency of the FM signal is the derivative of the angle, $\psi(t)$:

$$\frac{d\psi(t)}{dt} = \frac{d[\omega t + C\theta(t) + \beta}{dt} = \omega + c\frac{d\theta(t)}{dt}.$$

The frequency, ω, is being modulated by the time-varying signal x(t), given by:

$$x(t) = \frac{d\theta(t)}{dt} \text{ or } \theta(t) = \int^{t} x(s)ds.$$

The modulation index governs the magnitude of the modulating term which, in most applications, is smaller than the carrier frequency. Such an FM signal will have its instantaneous frequency varying about its carrier frequency. A large modulation index can cause the signal frequency to deviate from its carrier frequency to an extent that it may distort the signal. This is known as over-modulation.

The effect created by texture mapping the flow field requires that input textures are deformed along the flow directions such that the textures become enlongated with larger flow amplitudes and shortened with smaller amplitudes. This effect can be achieved by using an FM signal to map the textures as follows. Note that the value of an FM signal alternates periodically, and the rate of change is dependent on its instantaneous frequency. Thus, if the frequency is modulated by the flow amplitude, the amplitude of the FM signal will exhibit the same variation pattern as that of the flow speed. It is desirable that the larger speeds be mapped into enlongated textures. In terms of the FM signal, this corresponds to a slower rate of change. Thus, we need to modulate the FM frequency with a time-varying function which is inversely proportional to the speed.

The algorithm can be described by the following pseudo-code:

Inputs: N streamlines of various length computed in the image domain with instantaneous speed (flow amplitude) recorded at each node, carrier frequency w, and modulation index C;

Normalize the speed;
for j=1 to N do
Compute colors for each node k as
color[j][k] = cos(wt + C(1-speed[j][k]) + b).0.5+1,

end for
where t is the line integral from the node[j][0] to node[j][k] and β is a random initial phase in $[0,2\pi]$.

The texture color is a mapping of the FM signal amplitude and varies between 0 and 1. Since the algorithm computes the texture for each pixel along streamlines according to the FM signal without image composition, the input streamlines are required to cover the whole image domain without overlapping. Otherwise, signal interference will occur and damage the patterns. On the other hand, to obtain the best modulation, the streamlines should be as long as possible. To meet this, the following algorithm is used to generate the streamlines:

Inputs: flow field, minimum length L
Sub-divide the flow field into small cells such that each cell corresponds to a pixel in the output image;
Create streamlines starting from each cell;
Sort the streamlines from maximum length to minimum length and delete streamlines that shorter than L -> N streamlines of at least L long
Reset cell mask to zeros
for j=1 to N do
Check the cells that the streamline[j] passes
if no cells marked, then mark these cells traveled by streamline[j]
else if all cells already marked, discard streamline[j]
else break streamline[j] into small streamlines according to the cell mask, discard those shorter than L and insert the rest into the streamline array according to their length, delete streamline[j]
and adjust N
end for

An adaptive time increment 'nt' is used in the streamline integration to ensure the distance between adjacent nodes of the streamline is about the same length and cell size. Thus, the streamline length can be approximated by the number of nodes. The final cell coverage depends on the minimum length L. This constraint is used to eliminate short streamlines that will not have the contribution to the final texture. If L is chosen to be one, all cells will be covered.

RESULTS:

Figure 8 shows results from three different flow fields depicted at different resolutions. Figure 8a depicts a synthetic circular flow field of 280 x 280 pixels. The flow amplitude monotonically increases from the center to the outside. Figure 8b shows a horizontal wind field. The original flow field has a lower resolution than the image (264 x 210). The larger wind speed is in the middle of the field causing the enlongated texture patterns. Two cyclone centers are easily

visible. Figure 8c illustrates the top layer output of an ocean circulation model of the Gulf of Mexico. It features large ring structures and many small turbulent flows. Since it is merely a demonstration of the effectiveness of our FM-based algorithm, we chose not to perform any subdivision. Each pixel corresponds to a cell in the field with 194 x 146 cells. A minimum length of 5 was used in creating the streamlines for the wind and the current fields, resulting in a small number of pixels not being covered by the streamlines, but instead were assigned the background color.

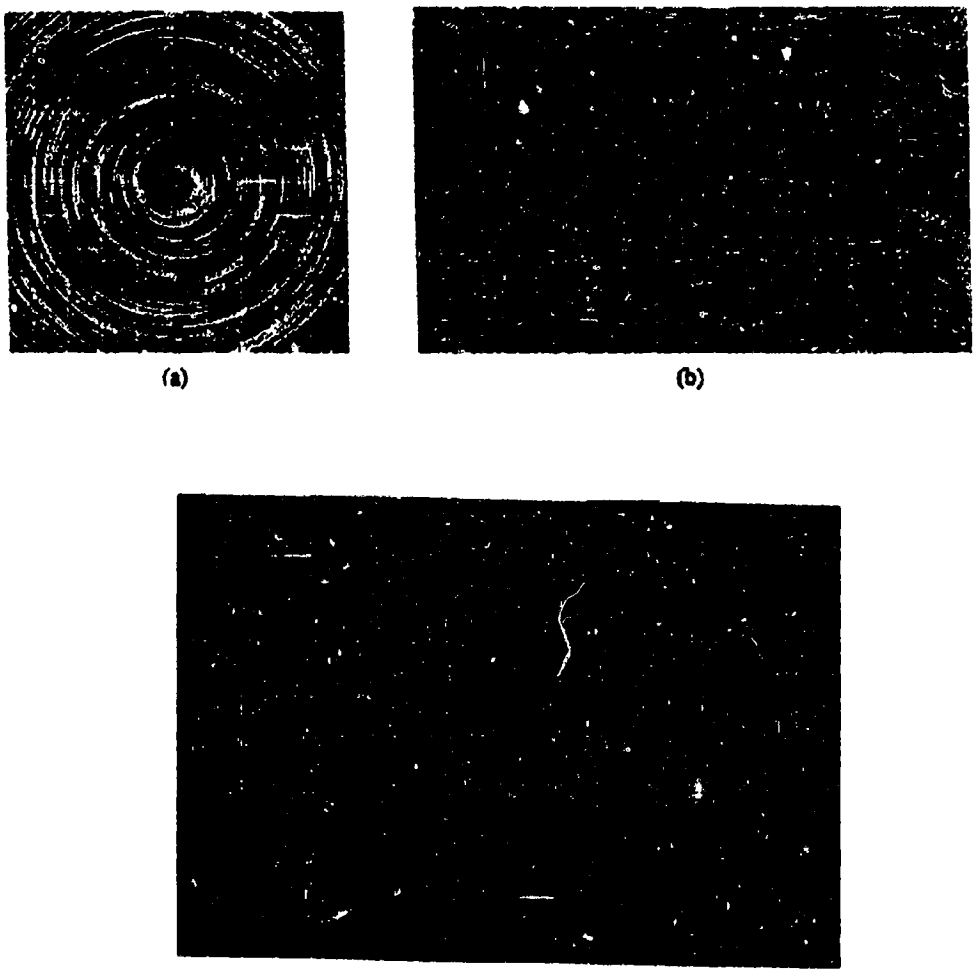

Figure 8. FM Texture mapping: a) a synthetic circular flow field of 280 x 280, b) a horizontal wind field of 264 x 210, and c) an ocean circulation field of 194 x 146.

Comparing the results, the circular flow field has the best effect. This is because the field is a perfect circular flow. There is no flow convergence or divergence. So, except for the four corners, all streamlines are complete circles. The texture of the wind field also displays a quality flow image. The textures in the middle exhibit enlongated patterns due to the larger wind velocities; the areas with slower speeds at the upper-left corner and near the bottom have shorter texture patterns. However, some discontinuities can be found in the areas with convergence and divergence. Particularly in regions where divergence occurs (to the right of the upper_cyclone center), such discontinuities are easily noticeable. This is because many new streamlines are started there to fill the decompressed area, and the texture colors at the beginning of those streamlines are decided by the random phases, producing abrupt effects. The texture image for the ocean circulation field has the lowest resolution in the three examples but much more flow turbulence. As a result, the created streamlines consist of more short pieces, and the minimum length constraint left relatively larger portion of pixels uncovered. Even so, the texture is still able to show the flow patterns of the eddies with various flow amplitudes.

FUTURE RESEARCH:

The main computation of the algorithm is in sorting and reorganizing the streamlines to eliminate overlap and to keep them with maximum possible lengths. The current algorithm used to create such streamlines is virtually a brute-force method, and further efforts are required. Once the global streamlines are generated, the mapping is quick. This allows easy modification of mapping parameters, and hence gives the algorithm the desired flexibility and control. Further research will also be directed at how to smooth the signal abruptness at the two ends of the streamlines. Such abruptness occurs because the signal/texture is only continuous within the streamline, and the signal at the first point of a streamline is determined by a random phase b. This is particularly problematic in large compression and decompression areas.

DISTRIBUTION LIST

1. Scientific Officer (Code 1242)
   Dr. Tom Curtin (3 Copies)
   Office of Naval Research
   800 N. Quincy Street
   Arlington, VA 22217-5000

2. Dr. Emmanuel Fiaderio
   Office of Naval Research
   800 N. Quincy Street
   Arlington, VA 22217-5000

3. Defense Technical Information Ctr
   Bldg 5, Cameron Station (2 Copies)
   Alexandria, VA 22304-6145

4. Administrative Grants Officer
   ONR Regional Office
   101 Marietta Street-Suite 2805
   Atlanta, GA 30303

5. Director, Naval Research Lab
   Attention: Code 2627
   Washington, DC 20375

6. Technical Director
   Oceanographer of the Navy
   U.S. Naval Observatory
   Washington, DC 20392

7. Director, Ocean Dynamics and
   Prediction Branch
   Naval Research Laboratory
   Stennis Space Center, MS 39529

8. Technical Director
   Commander Naval Meteorology and
   Oceanography Command
   Stennis Space Center, MS 39529

9. Naval Oceanographic Office
   Stennis Space Center, MS 39529
   -Mr. Landry Bernard
   -Dr. Martha Head

10. Chairman, Oceanography Dept.
    Naval Postgraduate School
    Monterey, CA 93943

11. Technical Director,
    Fleet Numerical Meteorology
    and Oceanography Center
    Monterey, CA 93943-5000

12. Space and Naval Warfare Systems
    Command (PMW175-3B)
    2451 Crystal Drive
    Arlington, VA 22245-5200
    -CDR Tim Sheridan
    -Dr. Edward Harrison

13. MSU Office of Research
    Mississippi State, MS 39762
    -Dr. Ralph Powe
    -Dr. Melvin Ray

14. MSU-NSF ERC
    P.O. Box 9726
    Mississippi State, MS 39762
    - Dr. Robert Moorhead

15. Center for Air Sea Technology
    Mississippi State University
    Building 1103 - Room 233
    SSC, MS 39529-6000
    -Mr. Valentine Anantharaj
    -Mr. James Corbin
    -Dr. David Dietrich
    -Dr. Avichal Mehra
    -Dr. Lanny Yeske
    -Dr. Zhifan Zhu

REPORT DOCUMENTATION PAGE

Form Approved OMB No. 0704-0188

1. Agency Use Only *(Leave blank).*	2. Report Date.	3. Report Type and Dates Covered.
	1 DECEMBER 1996	TECHNICAL REPORT 1 OCT 1995-30 SEPT 1996

4. Title and Subtitle.

FY96 POSTDOCTORAL ASSISTANT RESEARCH PROJECTS

5. Funding Numbers.

Program Element No.

Project No.

Task No.

Accession No.

6. Author(s).

A. MEHRA, Z. ZHU, AND L.A. YESKE (editor)

7. Performing Organization Name(s) and Address(es).

MISSISSIPPI STATE UNIVERSITY
CENTER FOR AIR SEA TECHNOLOGY
BUILDING 1103, ROOM 233
STENNIS SPACE CENTER, MS 39529

8. Performing Organization Report Number.

CAST TECHNICAL REPORT 1-97

9. Sponsoring/Monitoring Agency Name(s) and Address(es).

OFFICE OF NAVAL RESEARCH (CODE 1242)
800 NORTH QUINCY STREET, ARLINGTON, VA 22217
SPACE & NAVAL WARFARE SYSTEMS COMMAND, ARLINGTON, VA 22245
NAVAL RESEARCH LABORATORY, STENNIS SPACE CENTER, MS 39529
NASA, STENNIS SPACE CENTER, MS 39529

10. Sponsoring/Monitoring Agency Report Number.

CAST TECHNICAL REPORT 1-97

11. Supplementary Notes. Research performed under ONR Grants N00014-95-1-0186 and N00014-95-1-0293; NASA NAS13-564 Delivery Order 73; and through the DOD Advanced Research Projects Agency Strategic Environmental Research and Development Program under MSU-NSF Engineering Research Contract EEC-8907070.

12a. Distribution/Availability Statement.

Approved for public release; distribution is unlimited

12b. Distribution Code.

13. Abstract *(Maximum 200 words).*

Several FY1996 postdoctoral assistant research projects were conducted by Mississippi State University. This technical report describes these projects which include research on High Resolution Coastal Studies, Relocatable Numerical Models, Eddy Dynamics in Navy Layered Pacific Ocean Model Data, and Environmental Data Visualization System.

14. Subject Terms.

(U) Technical Report (U) Postdoctoral (U) Research (U) GUI (U) DieCAST (U) RME (U) DAMEE (U) ENVIS (U) UASVS

15. Number of Pages. 46

16. Price Code.

17. Security Classification of Report.	18. Security Classification of This Page.	19. Security Classification of Abstract.	20. Limitation of Abstract.
UNCLASSIFIED	UNCLASSIFIED	UNCLASSIFIED	